

**Südöstlicher Atlantik und südwestlicher Indik:
Rekonstruktion der sedimentären und tektonischen
Entwicklung seit der Kreide
AISTEK-I: Agulhas Transect**

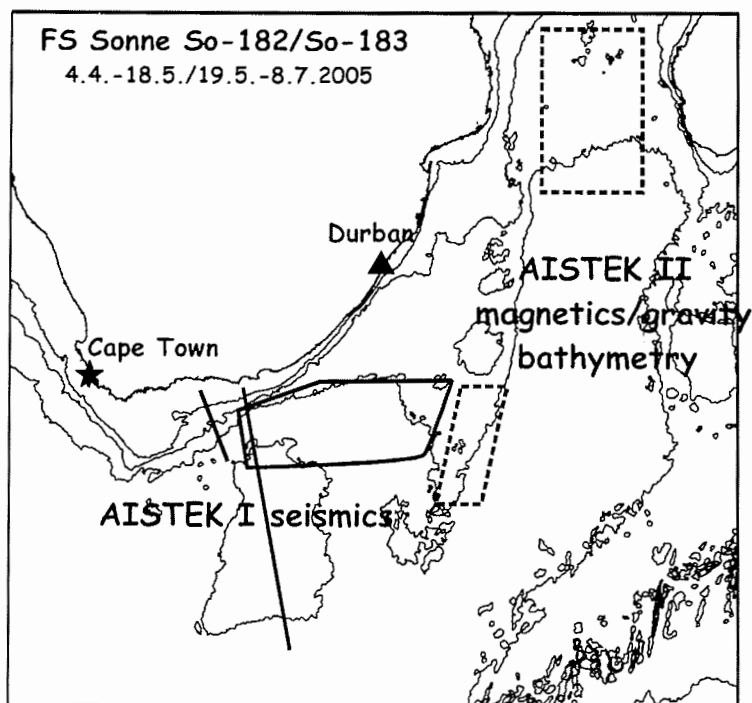
**Southeastern Atlantic and southwestern Indian Ocean:
reconstruction of the sedimentary and tectonic
development since the Cretaceous
AISTEK-I: Agulhas Transect**

Report of the RV "SONNE" cruise SO-182, Project AISTEK-I
4 April to 18 May 2005

**Edited by Gabriele Uenzelmann-Neben
with contributions from the Scientific Party of SO-182**

**Ber. Polarforsch. Meeresforsch. 515 (2005)
ISSN 1618 - 3193**

BMBF Förderkennzeichen 03G0182A



Gabriele Uenzelmann-Neben

Alfred-Wegener-Institut für Polar- und Meeresforschung
FB Geosystem
Am Alten Hafen 26
D-27568 Bremerhaven
Germany

guenzelmann@awi-bremerhaven.de

Contents

	Page
1. Zusammenfassung/Summary	5
2. Participants	8
2.1 Ship's crew	8
2.2 Shipboard scientific party	8
2.3 Participating organisations	9
3. Tectonic and geological framework	10
3.1 Tectonic evolution	11
3.2 Sedimentation and oceanic currents	13
4. Scientific objectives of AISTEK-I	15
4.1 Agulhas-Karoo Geoscience Transect	15
4.2 Sedimentation patterns in the Transkei Basin	16
5. Cruise itinerary	18
6. Navigation and DVS	23
7. Swath bathymetry (SIMRAD)	24
7.1 Method and instrument	24
7.2 Data processing	24
7.3 Preliminary results	24
8. Sediment echosounding (PARASOUND)	26
8.1 Instrument and processing	26
8.2 PARASOUND preliminary results	27
9. Seismics	37
9.1 Methods	37
9.2 Seismic equipment	37
9.2.1 Seismic sources, triggering and timing	37
9.2.2 Ocean-bottom seismometer/hydrophone systems (OBS/OBH)	40
9.2.3 Land-based seismic recorders and shots	42
9.2.4 Multi-channel reflection recording system	43
9.3 Processing of multi-channel reflection data	45
9.4 Preliminary results of multi-channel reflection data	45
9.4.1 The Agulhas Transect	46

9.4.2 The Transkei Basin	46
9.4.3 The Mozambique Ridge	48
9.5 Processing of refraction/wide-angle OBS/OBH data	49
9.6 Quality and preliminary results of refraction/wide-angle OBS data	50
10. Acknowledgements	53
11. References	54
Appendices	
App. I Seismic profile parameters	59
App. II OBS station list, profile AWI-20050100	61
App. III Land station and shot list, profile AWI-20050100	63
App. IV OBS station list, profile AWI-20050200	66
App. V Land station and shot list, profile AWI-20050200	69
App. VI OBS station list, profile AWI-20050300	72

List of Figures

- Fig. 1.1 RV Sonne So-182 cruise track map with seismic lines, and OBS/seismic land stations indicated. The dark lines on the Agulhas Plateau show the seismic lines collected in 1998, and the dark lines on the Agulhas Bank represent industry data. AB= Agulhas Bank, AP= Agulhas Plateau, NV= MR= Mozambique Ridge, Natal Valley, TB= Transkei Basin.
- Fig. 3.1 Tectonic units of southern Africa (from Frimmel, in press) and dominant structural features in the adjacent ocean basins as observed from the satellite-derived gravity anomaly grid of Sandwell & Smith (1997). Abbreviations: CFB - Cape Fold Belt, AB - Agulhas Bank, OB - Outeniqua Basin.
- Fig. 3.2 The Beattie Magnetic Anomaly (white dots) and the Southern Cape Conductive Belt (SCCB, black and white dashed lines) are continental scale geophysical anomalies. They stretch from east to west for more than 1000 km across southern South Africa.
- Fig. 7.1 Bathymetric map of all cruise lines during So-182.
- Fig. 8.1 Shown are all ship tracks recorded during So-182; thick lines mark the profiles which are discussed in this chapter. GEBCO bathymetry is used.
- Fig. 8.2 Shown is the shelf area of profile AWI-20050100; (1) marks the position of sediment lenses. Tilted sediment basement (2) and erosional channel can be observed (3).
- Fig. 8.3 A strong reflector (1) marks the base of a large sediment accumulation (2). Gravitational mass flow events (3) and wavy sediment pattern (4) are monitored on top of this sediment body.
- Fig. 8.4 This profile shows locations of channel systems (1, 2) and a flat terrace (3).
- Fig. 8.5 Lower slope area is characterized by a rough topography (1). In contrast upper slope show no sediment cover and a steeper slope angle (2). Single outcrop marks northern end of Agulhas Plateau (3). Sediment cover increases on top of the Agulhas plateau along this profile (4).
- Fig. 8.6 This profile shows the rough topography of the Agulhas Plateau including a large channel system as a characteristic feature (1).
- Fig. 8.7 PARASOUND profile recorded along reflection seismic line AWI-20050001.
- Fig. 8.8 Along profile AWI-20050003 a large sediment body could be observed. The upper figure shows the entire structure whereas only the southern part is seen in the lower figure.

- Fig. 8.9 Along profile AWI-20050007 a large sediment drift can be identified.
- Fig. 9.1 Principles of marine seismic reflection and refraction surveying.
- Fig. 9.2 Configuration of the different seismic sources used for seismic profiling.
- Fig. 9.3 Fig. 9.3: The three different airgun configuration used during the cruise: 3 GI-guns (above), 8 G-guns (middle), and the 32 l Bolt airgun (below).
- Fig. 9.4 IFM-GEOMAR OBH system (left) and OBS 3-foot (right) before deployment.
- Fig. 9.5 IFM-GEOMAR OBS flat system before deployment.
- Fig. 9.6 SERCEL SEAL™ digital multichannel seismic system provided by Exploration Electronics Ltd. and the recordings units.
- Fig. 9.7 Satellite derived topography (Smith and Sandwell, 1997) of the area of investigation showing the seismic lines acquired during this cruise in red. Red dots refer to the locations of the ocean bottom seismometers, and black dots to the locations of the land shots.
- Fig. 9.8 Part of line AWI-20050201 showing the Agulhas Passage. Note the sediment drift located in the northern part of the passage. This is a Constant-Offset plot without any gain applied.
- Fig. 9.9 Part of line AWI-20050201 showing a basement high a sedimentary basin on the central Agulhas Plateau. This is a Constant-Offset plot with no gain applied.
- Fig. 9.10 Line AWI-20050010 showing the Agulhas Drift. This is a Constant-Offset plot with no gain applied.
- Fig. 9.11 W-E cross section across the Agulhas Drift showing an older sediment drift underneath. This is a Constant-Offset plot with no gain applied.
- Fig. 9.12 Line AWI-20050301 from the Transkei Basin onto the Mozambique Ridge. This is a Constant-Offset plot with no gain applied.
- Fig. 9.13 Example of OBS data from line AWI-20050100, station 110 on the continental slope.
- Fig. 9.14 Example of OBS data from line AWI-20050200, station 204 on the Agulhas Plateau
- Fig. 9.15 Example of OBS data from line AWI-20050200, station 224 on the Agulhas Bank.
- Fig. 9.16 Example for OBS data from line AWI-20050300, station 304 on the southern Mozambique Ridge.

1. Zusammenfassung/Summary

Der FS „Sonne“-Fahrtabschnitt So-182 des Projektes AISTEK-I vom 4.4. bis 18.5.2005 bestand aus einem reflexions-refraktionsseismischen Messprogramm entlang eines Transects vom Festland und Schelf Südafrikas über die den Schelf begrenzende Agulhas Fracture Zone, über das Transkei Becken, das Agulhas Plateau bis in die Tiefsee westlich des Plateaus. Mit tiefenseismischen Methoden entlang dieses Transects und in benachbarten Gebieten sollten Daten gewonnen werden, die die geodynamischen Prozesse und die plattentektonischen Entwicklung der Region seit der Kreide beschreiben und modellieren lassen. Hochauflösende seismische Reflexionsdaten und sedimentechografische Aufzeichnungen vor allem des nördlichen Agulhas Plateaus und des Transkei Beckens lassen Hinweise auf die Veränderungen des Wassermassenaustauschs seit Öffnung des Seeweges zwischen Afrika und der Antarktis erwarten.

Auf diesem Fahrtabschnitt sind folgende Untersuchungsschwerpunkte bearbeitet worden:

- (1) *Die Untersuchung des tektonisch-strukturellen Aufbaus und der geodynamischen Entwicklung des Agulhas-Falkland Fracture Zone, der Agulhas Passage und des nördlichen Agulhas Plateaus:* Dieser Fragestellung wurde mittels zwei refraktionsseismischer Profile vom Schelf über das Outeniqua Becken, die Agulhas-Falkland Fracture Zone, die Agulhas Passage auf das Agulhas Plateau nachgegangen. So erhalten wir Aufschluss über die Beschaffenheit der Krustenstruktur in diesen tektonischen Einheiten als Basis für eine Modellierung ihrer geodynamischen Entwicklung seit dem Aufbruch Gondwanas.
- (2) *Entwicklung des Wassermassenaustausch zwischen dem Atlantik und dem Indik:* Eine reflexionsseismische Untersuchung des Transkei Becken, dessen Sedimentstrukturen durch die westsetzende Agulhas Strömung und die ostsetzenden Strömungen Antarktisches Bodenwasser und Nordatlantisches Tiefenwasser geprägt werden, wird hier Veränderungen in den Ablagerungsbedingungen und somit Hinweise auf die Chemie der Wassermassen und ihrer Pfade ergeben. So lassen sich Informationen über erstes Auftreten bestimmter Wassermassen und Modifizierungen ihrer Parameter erarbeiten, die dann Eingang in ozeanographische Modellierungen finden werden.

Insgesamt sind auf diesem Fahrtabschnitt 4230 km reflexionsseismische Profildaten, 1286 km refraktionsseismische Profildaten (mit 57 OBS- und 45 Landstationen) und ca. 11500 km fächerbathymetrische und sedimentechografische Daten registriert worden.

The RV "Sonne" cruise So-182, project AISTEK-I, took place from April 4th 2005 to May 18th 2005 and consisted of a seismic reflection and refraction survey along a transect from the South African continent across the shelf, the Agulhas-Falkland Fracture Zone, the Transkei Basin, the Agulhas Plateau into the deep sea. Deep seismic sounding along this transect and into neighbouring areas should produce data, which would allow the description and modelling of the geodynamic processes and plate tectonic development since the Cretaceous. High resolution seismic reflection data as well as sediment echosounding data will lead to indications for the modifications in water mass exchange since the opening of the gateway south of South Africa.

The leg consisted of the following main work programs:

- (1) *Investigation of the tectonic structure and geodynamic evolution of the Agulhas-Falkland Fracture Zone, the Agulhas Passage, and the northern Agulhas Plateau* by means of two deep seismic traverses from the shelf across the Outeniqua Basin, the Agulhas-Falkland Fracture Zone, the Agulhas Passage onto the Agulhas Plateau. In addition to acquiring seismic reflection multi-channel data, ocean-bottom seismographs (OBS) were deployed and provided detailed wave field information about the seismic velocity distribution and physical properties of the crust and upper mantle as a base for the modelling of the geodynamic development since the break-up of Gondwana.
- (2) *Evolution of the water mass exchange between the Atlantic and the Indian Ocean*: A seismic reflection investigation of the Transkei Basin, whose sedimentary structures are formed by the west setting Agulhas Current and the east setting Antarctic Bottomwater and North Atlantic Deep water, will show modifications in the depositional environment and thus the chemistry and paths of the water masses. This will lead to information on the first appearance of certain water masses and modifications of their parameters, which will be the base for oceanographic modelling.

In total, 4230 km of seismic reflection data, 1286 km of seismic refraction data (with 57 OBS and 45 land stations), and about 11,500 km of swath-bathymetric and sub-bottom profiler data were collected during this leg.

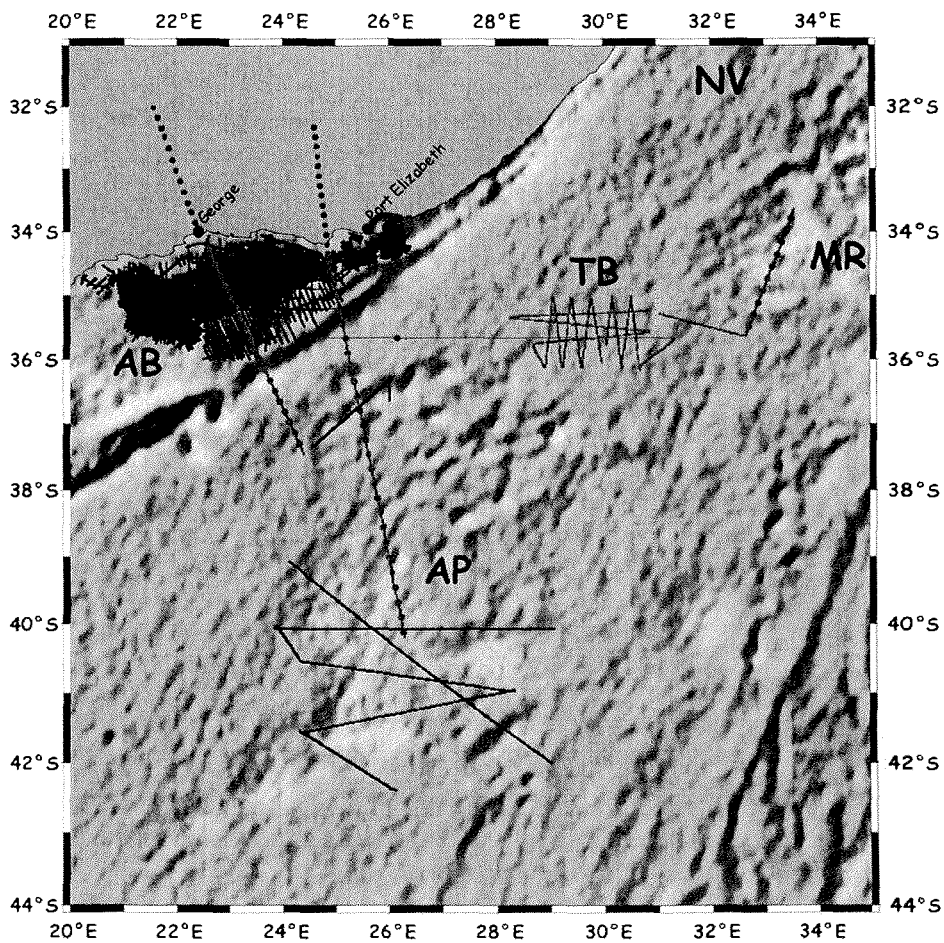


Fig. 1.1: RV Sonne So-182 cruise track map with seismic lines, and OBS/seismic land stations indicated. The dark lines on the Agulhas Plateau show the seismic lines collected in 1998, and the dark lines on the Agulhas Bank represent industry data. AB= Agulhas Bank, AP= Agulhas Plateau, NV= MR= Mozambique Ridge, Natal Valley, TB= Transkei Basin.

2. Participants

2.1 Ship's crew

Lutz Mallon	Master
Detlev Korte	Chief Officer
Nils-Arne Aden	1st Officer
Torsten Kowitz	2nd Officer
Heinrich Kolb	Surgeon
Norman Lindhorst	Chief Engineer
Andreas Rex	2nd Engineer
Klaus Dieter Klinder	2nd Engineer
Uwe Rieper	Electrician
Wolf-Hilmar Hoffmann	Chief Electronic Engineer
Jörg Leppin	System Operator
Katja Pfeiffer	System Operator
Rainer Rosemeyer	Fitter
Daniel Golabowski	Motorman
Frank Sebastian	Motorman
Wilhelm Wieden	Chief Cook
Seweryn Jastrzebski	2nd Cook
Gerlinde Gruebe	Chief Steward
Tomasz Majka	2 nd Steward
Hans-Peter Mucke	Bosun
Andreas Schrapel	A. B.
Jürgen Kraft	A. B.
Werner Hödl	A. B.
Detlef Etzdorf	A. B.
Torsten Biestedt	A. B.
Maurice Saathoff	A. B.
Dirk Dehne	A. B.

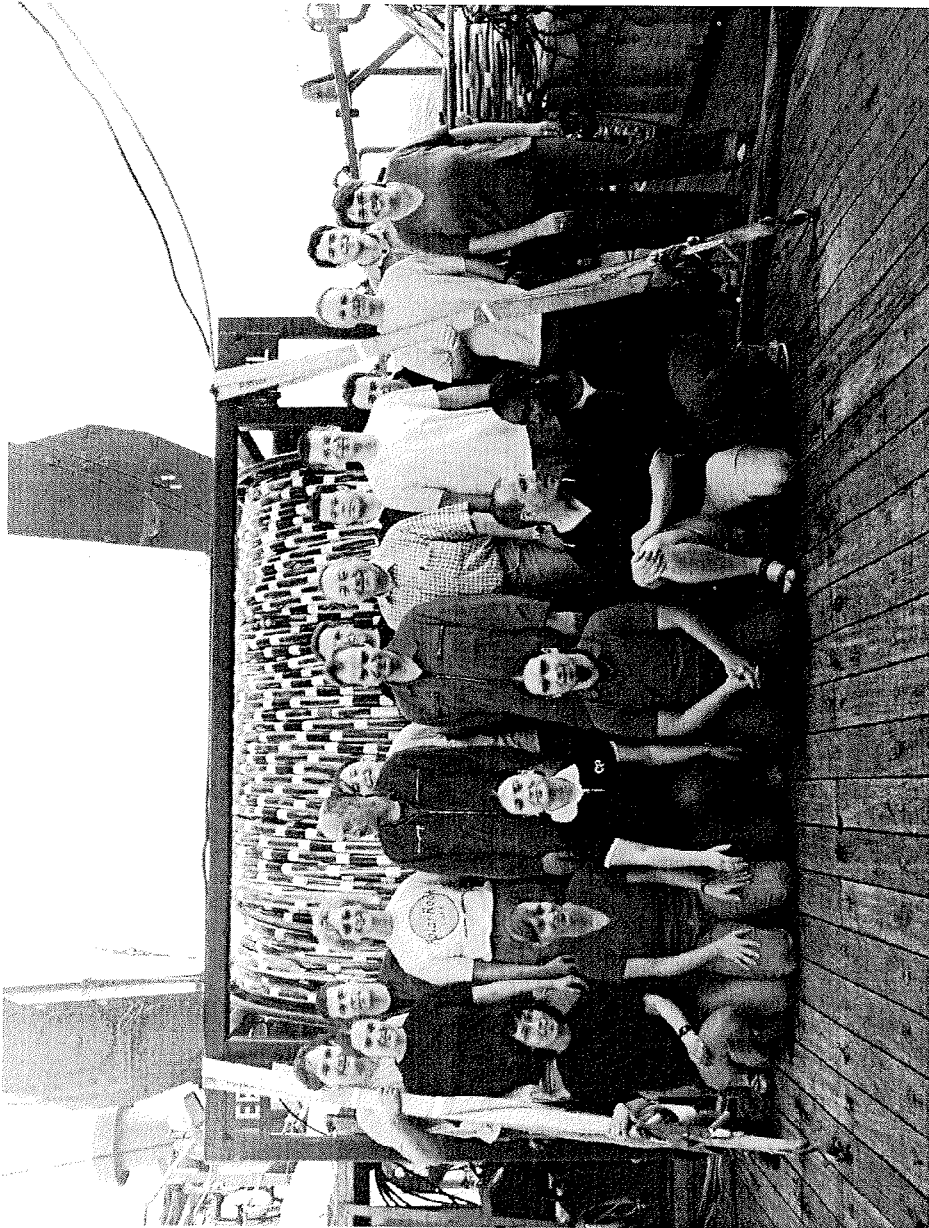
2.2 Shipboard scientific party

Gabriele Uenzelmann-Neben (chief scientist)	seismics	AWI
Karsten Gohl	seismics	AWI
Philip Schlüter	seismics	AWI
Graeme Eagles	seismics	AWI
Estella Weigelt	seismics	AWI
Catalina Gebhardt	seismics	AWI
Andre Gebauer	seismics	AWI
Simon Schneider	seismics	AWI
Norbert Lensch	seismics	AWI
Steven James Sibthorp	seismics	EEL

Kevin Coldham	seismics	EEL
Erik Lanbahn	OBS seismics	KUM
Christian Nettling	OBS seismics	KUM
Nicole Parsiegla	OBS seismics	AWI
Jan Grobys	OBS seismics	AWI
Daniela Berger	OBS seismics	AWI
Andre Fahl	OBS seismics	AWI
Katrin Huhn	Simrad/Parasound	RCOM
Katja Zimmermann	Simrad/Parasound	AWI
Tshifhiwa Mabidi	Simrad/Parasound	UCT
Robert Horn	Observer	CapFish

2.3 Participating organisations

- AWI Alfred Wegener Institute for Polar and Marine Research,
Columbusstrasse, D-27568 Bremerhaven, Germany
(www.awi-bremerhaven.de)
- EEL Exploration Electronics Ltd., Yarmouth Business Park, Suffolk Road,
Great Yarmouth, Norfolk NR31 0ER, United Kingdom
(info@exploration-electronics.co.uk)
- KUM UmweltMeerestechnik Kiel GmbH, Wischhofstr. 1-3, D-24148 Kiel,
Germany
(www.KUM.UmweltMeerestechnik.de)
- RCOM Research Center for Ocean Margins, University of Bremen, D-28334
Bremen
(www.uni-bremen.com)
- UCT Department of Geology, University of Cape Town, Rondebosch, 7700
Cape Town, South Africa
(www.uct.ac.za)
- CapFish Capricorn Fisheries Monitoring cc, Unit 15 Foregate Square, Table Bay
Boulevard, Cape Town, South Africa



3. Tectonic and geological framework

3.1 Tectonic evolution

(K. Gohl)

Onshore southern Africa offers an unrivalled region, where continental accretion processes over a period of more than 3.5 billion years can be studied (Fig. 3.1). A composite Archean (>2.5 Ga) craton (Kaalpvaal Craton) is flanked by progressively younger crust, recording four main stages of continental lithosphere formation: (1) the 2.06 - 1.80 Ga (Eburnian) Kheis Belt, (2) the 1.2 - 1.0 Ga (Grenvillian) Namaqua Natal Belt, (3) the 0.58 - 0.48 Ga (Pan-African) Saldania Belt and (4) the 0.25 Ga (Gondwanide) Cape Fold Belt (Frimmel, in press). Large areas of the Namaqua-Natal Belt are covered by Mesozoic Karoo sediments, and most of the Saldania Belt is overlain by rocks of the younger Cape Fold Belt (Frimmel et al., 2001). Only a few exposures in form of basins such as the Kangoo and the Kaaimans Inlier can provide reliable data on tectonism which are vital for the understanding of accretion and collision in southern South Africa. The southern margin of South Africa is the region where to best study the successive accretions of continental lithosphere onto the Kaapvaal Craton since its stabilization around 2.0 Ga. The same area also hosts two of Earth's largest known geophysical anomalies, the Beattie Magnetic Anomaly (BMA) and the Southern Cape Conductive Belt (SCCB). Both anomalies extend for almost 1000 km in east-west direction across southern South Africa (Fig. 3.2). The surface expressions of these anomalies seem to coincide with the mapped boundaries of the Cape Fold Belt and the Namaqua Natal Belt. The nature of both geophysical anomalies remains enigmatic. They have been interpreted as a slice of palaeo-oceanic lithosphere or alternatively as thrust zones, but neither their relative age nor their extent to depth and internal structure are known. A better understanding of their geometry and origin is essential for any meaningful reconstruction of the subsequent break-up processes.

Offshore, the geological situation is quite different. Apart from the near coastal shelf which might have been affected by the Cape Fold Belt deformation, the Gondwana break-up process of southern Africa, South America and Antarctica between 150 and 80 Ma characterized the continental shelf and its adjacent southwest Indian Ocean basin (Fig. 3.1). The sheared continental margin of southern Africa was formed when the Falkland Plateau of South America slid to the west leaving the dominant Agulhas-Falkland Fracture Zone (AFFZ) as a striking structural feature and a narrow and steep transition from the continental shelf to the oceanic crust of the Transkei Basin and Natal Valley (Ben-Avraham et al., 1993, 1997). The hydrocarbon-bearing Mesozoic Outeniqua Basin formed as a result of this translateral continental motion. A dense grid of exploration seismic lines and a number of drill sites provide the base for a structural and stratigraphic map of this basin and the Agulhas Bank (e.g. McMillan et al., 1997), but the deep crustal structure and its relationship to the geodynamic process of lithospheric translateral motion is still unknown. Farther south and southeast, the Agulhas Plateau and the Mozambique Ridge form large, bathymetrically elevated

regions of the southwest Indian Ocean whose nature and origin has implications for a better understanding of the Gondwana break-up process. The Agulhas Plateau is a Large Igneous Province (LIP) and consists most likely of overthickened oceanic crust formed at 120-100 Ma (Uenzelmann-Neben et al., 1999; Gohl & Uenzelmann-Neben, 2001). However, a few dredge samples of felsic composition from earlier studies point to a continental affinity of parts of the plateau (Allen & Tucholke, 1981; Tucholke et al., 1981; Ben-Avraham et al., 1995). Despite some geoscientific studies of the Mozambique Ridge (e.g. Lyakhovskiy et al., 1994; Ben-Avraham et al., 1995), its deep crustal nature and origin is still unknown, although plate-kinematic reconstruction models, which place it adjacent to the Astrid Ridge of Dronning Maud Land in Antarctica (Tikku et al., 2002; Jokat et al., 2003), as well as a few dredge samples (Mougenot et al., 1991; Ben-Avraham et al., 1995) rather imply a continental structure.

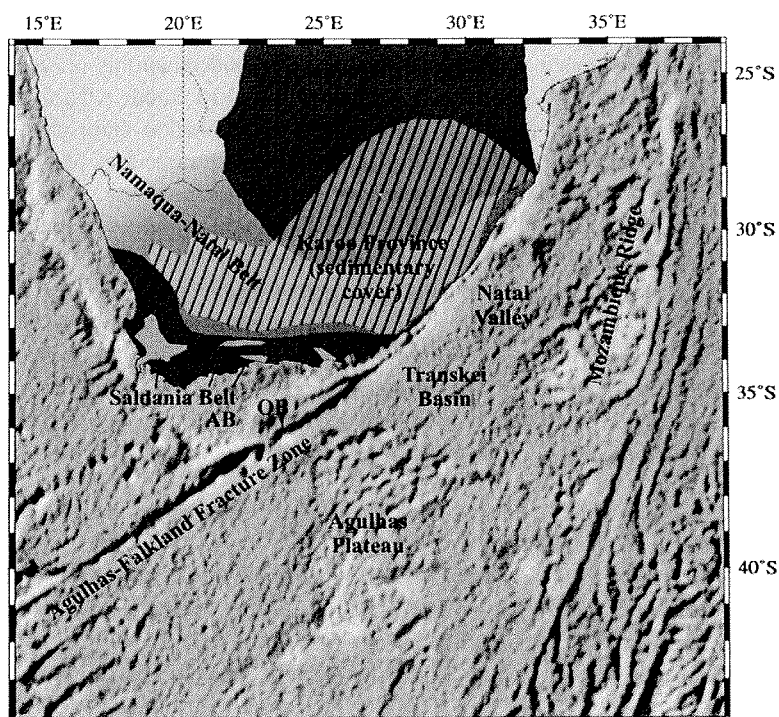


Fig. 3.1: Tectonic units of southern Africa (from Frimmel, in press) and dominant structural features in the adjacent ocean basins as observed from the satellite-derived gravity anomaly grid of Sandwell & Smith (1997). Abbreviations: CFB - Cape Fold Belt, AB - Agulhas Bank, OB - Outeniqua Basin.

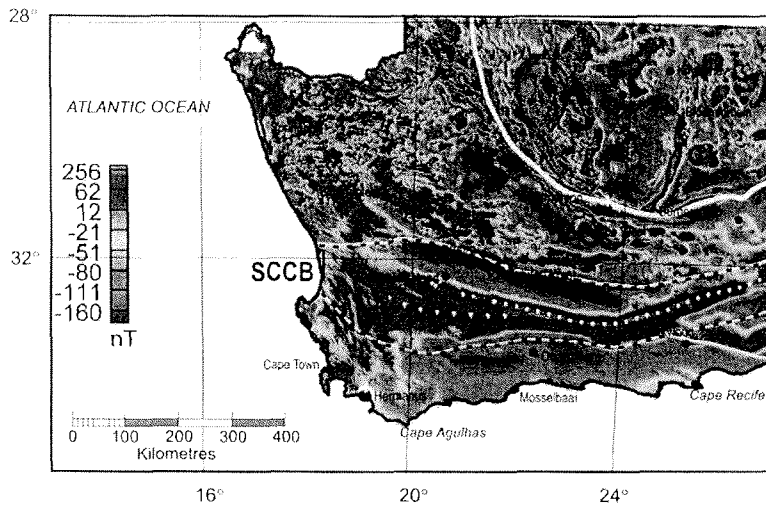


Fig. 3.2.: The Beattie Magnetic Anomaly (white dots) and the Southern Cape Conductive Belt (SCCB, black and white dashed lines) are continental scale geophysical anomalies. They stretch from east to west for more than 1000 km across southern South Africa.

3.2 Sedimentation and oceanic currents

(G. Uenzelmann-Neben)

Since the 70s the shelf and continental slope of South Africa have been of major interest for both academia (Dingle and Camden-Smith, 1979; Dingle et al., 1987; Ben-Avraham et al., 1995 and 1997; Niemi et al., 2000) and industry. This showed that the sedimentary sequences are distinctly characterised by erosion and re-sedimentation due to different current systems. The Agulhas Passage, an about 50 km long narrow, up to 4000 m deep depression between the South African continental margin and the Agulhas Plateau, was identified as the main passage of Antarctic Bottomwater (AABW) (Dingle and Camden-Smith, 1979; Camden-Smith et al., 1981). This led to erosion and deformation of the sediments.

The sedimentary cover of the Agulhas Plateau also shows the strong influence of AABW. Tucholke and Embley (1984) report an erosional zone, which surrounds the plateau. Tucholke and Carpenter (1977) and Tucholke and Embley (1984) identify four distinct horizons in their seismic single channel data and geological data, which they correlate with regional hiatus. Those comprise horizons as a result of a sea level highstand in combination with low sedimentation rates (Palaeocene/Eocene) or erosion due to modified currents (early/middle Oligocene: onset of Antarctic Circumpolar Current (ACC); middle Miocene: AABW; upper Miocene/lower Pliocene: Circumpolar Deepwater in the ACC). Based on the seismic reflection data of the SETARAP project carried out in 1998 a model could be developed, which shows the influence of the

different water masses in time and space on the sedimentary column on the southern Agulhas Plateau (Uenzelmann-Neben, 2001 and 2003). Thus we have indications for a water mass, which resembles the present day AABW and which re-deposited sediment on the south-western Agulhas Plateau as early as Eocene.

Little is known about the sedimentary cover of the northern Agulhas Plateau. Tucholke and Carpenter (1977) just acquired the general thickness. The transition into Agulhas Basin and Transkei Basin remains also unsettled. Are the flanks of the plateau characterised by slides and slumps? In what way do the contourites observed by Tucholke and Carpenter (1977), Tucholke and Embley (1984) and Uenzelmann-Neben (2001 and 2003) continue into the surrounding basins? We don't know whether AABW has been active on the northern Agulhas Plateau in Eocene times as reported for the southern plateau. This would have a distinct impact on the climate models and the ideas on the glaciation of Antarctica. Further, we know little about the initial occurrence and the paths of North Atlantic Deep Water (NADW) and the Agulhas Current/Retroflexion. But the interplay of those cold (deep) and warm (surface) water masses is of crucial importance for the development of the climate, e.g. the glaciation of Antarctica.

Sediment drifts were identified in the Natal and the northern Transkei Basins, which document the erosional and re-depositional processes due to bottomwater (Niemi et al., 2000). Niemi et al. (2000) concentrate on the sediment drifts in the Natal Basin while the detailed location and elongation of the Agulhas Drift (Transkei Basin) remains unknown. They define a seismostratigraphic concept, which comprises three main reflections. It remains vague how Niemi et al. (2000) correlate their concept with the work of Tucholke and Carpenter (1977), Tucholke and Embley (1984) and Uenzelmann-Neben (2001 and 2003). Taking into account the present day path of NADW and Agulhas Current we conclude that the Agulhas Drift represents a document of the development of those two water masses and hence enables the reconstruction of those currents's variation in time and space.

According to Ben-Avraham et al. (1994) the geostrophic currents flowed along the southwest African continental margin during the Oligocene. It now flows eastward in the Transkei Basin. As the reason for this modification Ben-Avraham et al. (1994) see the emergence of the Mozambique Ridge. This is an example for the influence changes in the seafloor topography in the southern Atlantic and Indian have on the global oceanic circulation (Ben-Avraham et al., 1994).

4. Scientific objectives of AISTEK-I

4.1 Agulhas-Karoo Geoscience Transect

(K. Gohl)

Southern Africa and its southern continental margin offer an unrivalled region, where continental accretion and break-up processes over a period of more than 3.5 billion years can be studied. Along a geoscientific transect, stretching from the offshore Agulhas Plateau across the Agulhas Fracture and the Outeniqua Basin, continuing across the Cape Fold Belt, the Namaqua-Natal Belt and into the Karoo Province and the southern Kaapvaal Craton, geophysical and geological/geochemical data and samples are collected in order to build a model of the evolution and crustal accretion as well as the continental break-up of this region. With such a single transect, multi-fold significant objectives can be addressed such as the Proterozoic accretion processes along the southern margin of the Kaapvaal Craton, the extent of Pan-African inliers in the Cape Fold Belt, the extent and formation of the Cape Fold Belt, the sources for the Beattie Magnetic Anomaly and the Southern Cape Conductivity Belt, the continental/oceanic origin of the Agulhas Plateau and the formation of the Agulhas Fracture Zone and its consequences for basin formation and uplift processes relevant for the hydrocarbon producing provinces of the Outeniqua Basin. A combined land-sea deep crustal seismic reflection and refraction survey as well as a magnetotelluric survey on land along the transect will provide detailed structures and constraints for physical parameters from the upper crust to the upper mantle which will be integrated with geological, petrological and geochemical analysis on rock composition, age and alteration history to form an overarching geodynamic model for the evolution of the region and its tectonic units. This transect is part of the German - South African collaborative geoscientific research programme "Inkaba ye Africa" (2003), Project 2.2 "*Agulhas-Karoo Geoscience Transect: A land-sea deep crustal seismic, MT and petrological transect across the Agulhas Plateau, the Agulhas Fracture Zone, the Agulhas Bank, the Cape Fold Belt and into the Karoo Province*".

The offshore component of this transect, which is part of the seismic survey program of SO-182, has the following objectives:

- (1) the nature of the Agulhas Plateau and Mozambique Ridge (oceanic versus continental) and the amount of magmatic material added to it at various times is a premier target of the offshore studies. Recent deep seismic surveying of the southern central Agulhas Plateau indicates very high P-wave velocities (>7 km/s) in the lower two-thirds of the 25 km thick crustal column, suggesting an oceanic crustal affinity. However, this is in conflict with the interpreted continental origin of quartzo-feldspathic samples dredged from the plateau. It is uncertain if the observed velocity-depth distribution is symptomatic for the entire plateau or if continental crustal fragments are embedded in the plateau. An important aim is to understand the role of young volcanism near the northern Agulhas Plateau.

- (2) origin of the Agulhas Fracture Zone and its relationship to the separation of the Falkland Plateau. Furthermore, the question of any magmatism having been associated with break-up and the tectonic as well as magmatic consequences of possible repeated re-activation of the fracture zone along the continental margin will be addressed. The key question is: Under what geodynamic process did the sheared margin of South Africa evolve?
- (3) on the Outeniqua Basin of the Agulhas Bank, the nature and position of the crust-mantle boundary as well as the development of the oil-producing sedimentary basin and its deep-seated fractures during break-up will be examined.
- (4) the extensional history of the Cape Fold Belt related to the break-up of Gondwana during the Mesozoic will form part of the study, where normal faults and related structures can be identified along the planned transect through the Cape Fold Belt.

In order to address these questions, two sub-parallel deep crustal seismic profiles have been planned along a marine transect from the Agulhas Plateau, across the Agulhas Fracture Zone and the Agulhas Bank toward the South Coast (Fig. seismic track map). While the western profile is primarily aimed for imaging the deep Outeniqua Basin and its transition into the Agulhas Fracture Zone, the eastern profile will reveal the structure of the narrow sheared continental margin and the nature of the Agulhas Plateau. A third deep crustal profile is planned to reveal the structure and composition of the adjacent southern Mozambique Ridge.

4.2 Sedimentation patterns in the Transkei Basin

(G. Uenzelmann-Neben)

The gateway south of South Africa is characterised by a number of oceanic current systems. These currents form part of the worldwide conveyor belt, which strongly influences Earth's climate. At the surface, the Agulhas Current sets from the Indian Ocean in the east towards the west thus transport heat into the Atlantic. In larger depths we find both North Atlantic Deep Water and Antarctic Intermediate Water, and near the bottom Antarctic Bottom Water. The Transkei Basin south of South Africa is a key area, where those water masses interact.

The development of the oceanic currents south of Africa is documented in the sedimentary sequences and units, which characterise that area. The investigation of those sedimentary sequences and units with high-resolution seismic reflection, sedimentological and geochemical methods will thus enable the answer of the following questions:

- (1) when did the exchange of water masses between the Atlantic and the Indian Oceans commence? Significant heat transfer can be observed in the seaway south of South Africa, which is of importance for the maintenance of the global

conveyor belt and thus the global climate. In this way the warm south setting Agulhas Current leads to a tropical climate in eastern Africa, while the cold north setting Benguela Current leads to arid climate in western Africa. Heat is being transported into the South Atlantic via Agulhas rings and eddies and can thus modify the Benguela Current (Richardson et al., 2002). It now remains to show when the heat transfer started in larger dimensions and whether short-term climate fluctuations had any effect on the general process.

- (2) when do we find first indications for aggressive, erosive water masses similar to present day NADW and AABW?
- (3) which effect did the opening of the gateway south of Africa have on production, transport and deposition of sediments?
- (4) which indications for modifications of AABW, NADW, ACC and/or Agulhas Current in time and space can we identify?

The Agulhas Plateau represents an immense obstacle for the path of oceanic currents south of Africa. Due to the rise of the seafloor to water depths of 1800 m and less the currents are channelled (a) through the Agulhas Passage in the north, or (b) led along the rather deep flanks of the plateau. In this way characteristic current induced sediment structures and distributions are generated, which allow the reconstruction of current paths and intensities in the various epochs. An example for this is the Agulhas Drift in the northern Transkei Basin, which is shaped by AABW, NADW and the Agulhas Current. But the exact location, elongation and age of the Agulhas Drift remain unknown. The development of the drift in time and space gives information on the first appearance of AABW, NADW and Agulhas Current in this area. On the southern Agulhas Plateau those information could only be compiled via seismic reflection investigations (Uenzelmann-Neben, 2001 and 2003).

A grid of high-resolution seismic reflection profiles in the Transkei Basin will lead to the identification of current induced sediment structures. Their extension will be mapped and thus give information on commencement and path of currents.

5. Cruise itinerary

(G. Uenzelmann-Neben)

Day	Date	Approx. Board Time	Activities; Work Program	Weather
Mo	04.04.	10:00	Cape Town harbour; loading, unpacking and installation of equipment;	fine
We	06.04.	09:00	departure from Cape Town; transfer towards first OBS profile; installation of equipment;	fine
Th	07.04.	08:00 13:40 - 18:45 22:10-	test deployment of streamer, extra streamer sections were added; test deployment of G-gun array and Bolt airgun; for shooting soft start was employed; seismic test recording went well; CTD and releaser test of OBS	fine higher swell fine fine
Fr	08.04.	02:26 07:53- 09:45 10:00	another releaser test; begin deployment of 20 OBS/OBH along Profile 20050100 from SE to NW (20 km spacing);	low swell medium winds
Sa	09.04.	05:27 06:26 09:25 10:40- 10:51 12:40- 1251 14:30- 14:35	end deployment of OBS/OBH; deployment of streamer, G-guns array and Bolt airgun; begin soft start; interruption of shooting due to a land shot; resume shooting with soft start; interruption of shooting due to a land shot; resume shooting with soft start; interruption of shooting due to a land shot; resume shooting with soft start	lower swell fine lower swell lower swell lower swell
Su	10.04.	06:30- 06:41 08:25- 08:36 08:50- 08:56 11:35- 11:45	interruption of shooting due to a land shot; resume shooting with soft start; interruption of shooting due to a land shot; resume shooting with soft start; interruption of shooting due to a land shot; resume shooting with soft start; interruption of shooting due to a land shot; resume shooting with soft start;	strong winds strong winds strong winds strong winds

		13:15- 13:20	interruption of shooting due to a land shot; resume shooting with soft start;	strong winds
		22:01 22:30 23:23 23:48	retrieval of broken Bolt airgun; retrieval of G-gun array; deployment of G-guns; begin soft start;	strong winds strong winds strong winds strong winds
Mo	11.04.	05:50- 06:00 07:40- 07:50 09:20 10:36 11:21- 14:12	interruption of shooting due to a land shot; resume shooting with soft start; interruption of shooting due to a land shot; resume shooting with soft start; end of profile 20050100; retrieval of G-guns; retrieval of streamer	strong winds, high waves very strong winds, high waves strong winds, high waves
Tu	12.04.	10:03-	retrieval of OBS/OBH;	good condition
We	13.04.	15:39	transit to start point of seismic reflection profiling;	good condition
Th	14.04.	02:10 03:53 04:12 04:30	deployment of streamer; deployment of GI-guns; begin soft start; start shooting profile 20050001	fine fine
Su	17.04.	08:02 09:58 18:44 21:09	end of profile 20050001; start of profile 20050002; end of profile 20050002; start of profile 20050003;	stronger winds; higher swell
Mo	18.04.	10:54 11:18 15:21 15:59	end of profile 20050003; retrieval of GI-guns and repairs; deployment of GI-guns; begin soft start; start of profile 20050004	higher swell higher swell
Tu	19.04.	04:37 06:26 07:25 07:50 07:57 19:50 21:43	end of profile 20050004; start of profile 20050005; retrieval of GI-guns and repairs; deployment of GI-guns; begin of soft start and resume shooting; end of profile 20050005; start of profile 20050006;	increasing wind and swell strong winds increasing winds and

				swell
We	20.04.	07:42 08:01 08:07	end of profile 20050006 due to extremely bad weather; retrieval of GI-guns; retrieval of streamer;	strong winds and high swell
Th	21.04.	07:30- 10:28	CTD and releaser test;	medium winds
Fr	22.04.	07:29-	deployment of 27 OBS/OBH along profile 20050200 from SE to NW;	fine
Sa	23.04.	14:48 15:25 17:00 17:11 17:34 18:00	deployment of streamer; deployment of G-gun array; deployment of Bolt airgun; begin soft start; start of profile 20050200; retrieval of Bolt airgun, which does not hold pressure;	increasing winds medium winds
Su	24.03.	04:39- 04:44 05:20- 05:25 09:00- 09:10 10:44 10:55- 11:04 14:20- 14:30 16:00- 16:10 23:46	interruption of shooting, because compressor is down; resume shooting with soft start; interruption of shooting, because compressor is down; resume shooting with soft start; interruption of shooting due to a land shot; resume shooting with soft start; deployment of Bolt airgun; interruption of shooting due to a land shot; resume shooting with soft start; interruption of shooting due to a land shot; resume shooting with soft start; interruption of shooting due to a land shot; resume shooting with soft start; interruption of shooting due to a land shot; resume shooting with soft start; retrieval of Bolt airgun because buoy was lost;	medium winds medium winds medium winds medium winds medium winds medium winds
Mo	25.04.	00:40 07:40- 07:50 09:10- 09:20 11:05- 11:15 13:05- 13:15	deployment of Bolt airgun; interruption of shooting due to a land shot; resume shooting with soft start; interruption of shooting due to a land shot; resume shooting with soft start; interruption of shooting due to a land shot; resume shooting with soft start; interruption of shooting due to a land shot; resume shooting with soft start;	medium swell, increasing winds; stronger winds
Tu	26.04.	07:45- 07:55 10:00-	interruption of shooting due to a land shot; resume shooting with soft start; interruption of shooting due to a land shot;	higher winds and swell

		10:10 11:55- 12:05 13:40- 13:50 14:55- 15:04	resume shooting with soft start; interruption of shooting due to a land shot; resume shooting with soft start; interruption of shooting due to a land shot; resume shooting with soft start; interruption of shooting due to a land shot; resume shooting with soft start;	
We	27.04.	01:04 01:14 01:49 01:51 05:45-	end of profile 20050200; retrieval of Bolt airgun; retrieval of G-guns; retrieval of streamer; retrieval of OBS/OBH	medium winds increasing winds
Fr	29.04.	08:30	transit to start point of seismic reflection profiles;	medium winds
Sa	30.04.	11:41 14:59 15:06	deployment of streamer; deployment of GI-guns; begin of soft start; start of profile 20050007	medium winds and swell
Su	01.05.	03:25 03:43 19:19 19:55	end of profile 20050007; start of profile 20050008; end of profile 20050008; start of profile 20050009	strong winds and swell
Mo	02.05.	08:32 08:51 22:12 22:53	end of profile 20050009; start of profile 20050010; end of profile 20050010; start of profile 20050011	medium winds
Tu	03.05.	01:14 03:19 14:39 14:53	stop shooting due to a shark bite in the streamer; repair of streamer; resume shooting with soft start; end of profile 20050011; start of profile 20050012	medium swell increasing winds decreasing winds
We	04.05.	04:12 04:33 09:24 09:44	end of profile 20050012; start of profile 20050013; end of profile 20050013 start of profile 20050014;	fine fine
Th	05.05.	08:03 08:21	end of profile 20050014; start of profile 20050015;	fine
Fr	06.05.	09:41 10:09	end of profile 20050015; start of profile 20050016	strong winds and high swell
Sa	07.05.	14:55	end of profile 20050016;	medium

		15:14 18:18 18:30 18:31 18:51	retrieval of GI-guns; battery change in streamer birds; deployment of streamer; deployment GI-guns; begin soft start; start of profile 20050017	swell
Su	08.05.	13:01 13:10	end of profile 20050017; start of profile 20050018; deployment of 10 OBS parallel to shooting of profile 20050018;	increasing winds and swell
Mo	09.05.	15:34 15:54 16:42 17:45 18:08 18:09 18:30	end of profile 20050018; retrieval of GI-guns; repair of shark bite on streamer; deployment of streamer; deployment of G-guns and Bolt airgun; begin of soft start; start of profile 20050300	medium swell fine
We	11.05.	02:28 03:00 03:15 03:17 08:22-	end of profile 20050300; retrieval of Bolt airgun; retrieval of G-guns; retrieval of streamer; retrieval of OBS	stronger winds and swell; strong winds and swell
Th	12.05.	00:48	transit to start of Parasound and Simrad survey;	very rough seas and high swell
Sa	14.05.	09:43	start of Parasound and Simrad survey;	fine
Su	15.05.	17:27	end of Parasound and Simrad survey;	very rough seas and high swell
Tu	17.05.	09:30	arrival in Cape Town harbour; packing and unloading of equipment	very rough and high swell
We	18.05.		Cape Town harbour; packing and unloading of equipment	

6. Navigation and Data Distribution System (DVS)

Accurate navigation coordinates are essential for geophysical surveying and geological sampling. RV Sonne is equipped with an ASHTEC differential Global Positioning System (D-GPS) with an accuracy of about 10 m. The navigation data were made available to the scientific groups through the ship's Data Distribution System (DVS) and downloaded in regular intervals as 1-minute- or 1-second-files onto the "wiss-data" directory which could be accessed on every on-board networked computer. Due to temporary failures of the Interface-Processor (IFP) for the DVS, the navigation files contain a number of data gaps, ranging from a few minutes to a few hours in one case. Beginning during the first IFP failure, we arranged for an DVS-independent recording of D-GPS coordinates during seismic profiling through an D-GPS interface connection to a PC notebook in the Geolabor.

7. Swath bathymetry (SIMRAD)

(K. Huhn and watch keepers)

7.1 Method and instruments

During the whole cruise a Kongsberg SIMRAD EM120 multibeam echosounder which is installed on RV SONNE was used for mapping the seafloor (EM120 Product Description.pdf). The seafloor is sampled by 191 beams of well known pre-defined angles. The beam width is 2x2 degree. It surveys the water depth using up to 150° opening angle. The system operates at a frequency of 12 kHz, subdivided into several transmitting transducer-sectors with 11.25 to 12.75 kHz and independent heave, pitch, roll compensator steering. The pulse length is 15 ms. Diameter of footprints of one single beam at 500 m water-depth is 17.5 m at the nadir, and 97 m for the outermost beam. At 3000 m water-depth, the footprints are 104 m and 587 m respectively. Due to the high number of beams, the distance between the beams at 3000m water-depth is 67 m. The system uses a calibration mode to calculate the position and depth for single beams of the sequentially send pings using installation angles, vessel attitude, and sound profile. The sound profile was obtained from a CTD cast. Transmitting and receiving units are separated.

The positioning was done with Realtime Differential GPS (Racal Skyfix). The accuracy is approximately 10 m for the first.

7.2 Data processing

Processing for the bathymetric data was carried out with the Neptune Software package by SIMRAD. Outer beams were zapped, artefacts were identified and flagged, depth errors can be corrected. Processing takes into account installation offsets and a sound velocity profile recorded two times during the cruise. In addition, SIMRAD EM120 measures the backscatter intensities. The data were imaged as contour plots with the GMT software package (Wessel and Smith, 1998) after gridding.

The SIMRAD multibeam was used on all surveys during R/V SONNE Cruise SO182 and was serviced by the PARASOUND operator on a 24-hour schedule.

During the entire cruise, GPS and DGPS were available and provided high quality navigation data.

7.3 Preliminary Results

The SIMRAD EM120 system was used during the entire cruise on all seismic profiles and transits between stations. During SO182 the system was run with 130° opening angle in deep mode because of the partly bad weather conditions. This generally results in isolated stripes of bathymetric data along the tracks (Fig. 7.1).

In addition a dense grid of profiles were recorded between 28.5°E - 31°E and -35°S -

-37°S. This data will be processed with the public domain software MultiBeam system to reduce artefacts (Caress and Chayes, 1996).

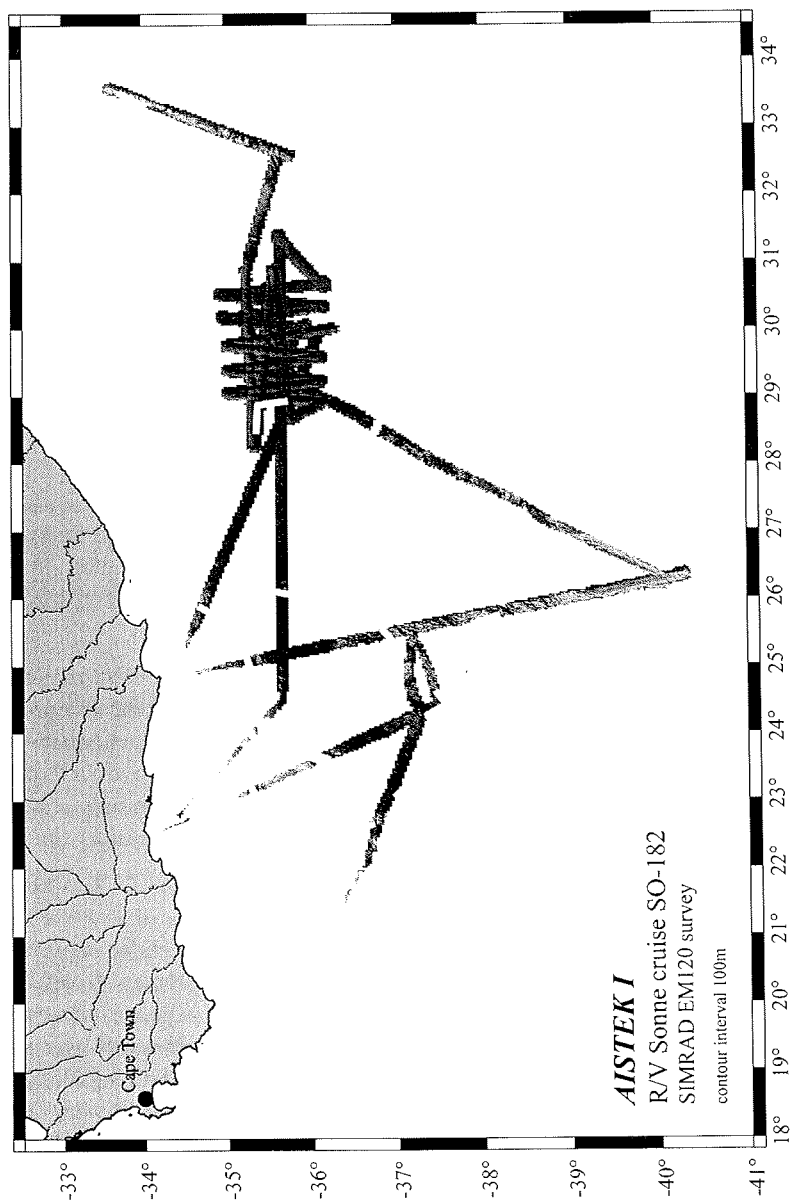


Fig. 7.1: Bathymetric map of all cruise lines during So-182.

8. Sediment echosounding (PARASOUND)

(K. Huhn, T. Mabidi, K. Zimmermann, S. Schneider, and watch keepers)

8.1 Instruments and processing

A Krupp Atlas PARASOUND system is permanently installed on RV SONNE. The PARASOUND system is a sub-bottom profiler or sediment echosounder. The hull-mounted transducer array has 128 elements on an area of $\sim 1 \text{ m}^2$. It requires up to 70 kW of electric power due to the low degree of efficiency of the parametric effect. In 2 electronic cabinets, beam forming, signal generation and the separation of primary (18, 22 kHz) and secondary frequencies (4 kHz) are carried out. The system is operated on a 24-hour schedule with the third electronic cabinet in the echosounder control room.

The PARASOUND system works as a low-frequency sediment echosounder as well as a high-frequency narrow beam sounder to determine water depths. This technique based on the parametric effect, which produces additional frequencies through nonlinear acoustic interaction of finite amplitude waves. If two sound waves of similar frequencies (here 18 kHz and e.g. 22 kHz) are emitted simultaneously, a signal of the difference frequency (e.g. 4 kHz) is generated for sufficiently high primary amplitudes. The new component is travelling within the emission cone of the original high frequency waves, which are limited to an angle of only 4° for the equipment used. The resulting footprint size of 7% of the water depth is much smaller than for conventional systems, and both vertical and lateral resolution is significantly improved.

A burst of pulses is sending out at 400 ms intervals until the first echo returns. The coverage of this discontinuous mode depends on the water depth, and produces non-equidistant shot distances between bursts. On average, one seismogram is recorded about every second providing a spatial resolution on the order of a few meters on seismic profiles at 6.0 knots. To reduce the amount of disk-space, only a 200 m depth / 266 ms time-window was recorded. The main tasks of the operators are system and quality control and to adjust the start of the reception window and keeping the seafloor in the upper half of the recording window.

Furthermore, RV SONNE is equipped with the digital data acquisition system PARADIGMA, which was developed at the University of Bremen (Spieß, 1993). The data were stored on two exchangeable disc drives of 4 gigabyte capacity, allowing continuous recording between several days dependent on water depth. The seismograms were sampled at a frequency of 40 kHz, with a typical registration length of 266 ms for a depth window of $\sim 200 \text{ m}$. During SO182 6 GB of PARASOUND data were recorded. The data format is in standard SEG-Y (Society of Exploration Geophysicists) -- format. The penetration depends on the seafloor properties. For soft sediments penetrations of 80m were observed on. Hard sediments reduce the penetration to few 10s of meters.

During the cruise, PARASOUND sections were plotted for all profiles. These plots give a first impression of variations in seafloor morphology, sediment coverage and

sedimentation patterns along the ship's track. In addition, an online processing was carried out for interesting areas eliminating most of the changes in window depth. The echogram sections were filtered with a wide band pass filter to improve the signal-to-noise ratio. In addition, the data were normalized to a constant value much smaller than the average maximum amplitude, thus amplifying deeper and weaker reflections.

The PARASOUND systems worked very well during the entire cruise under the very professional assistance by electricians of the vessel.

8.2 PARASOUND Preliminary Results

PARASOUND data were collected along all seismic profiles and transits between stations coevally to echosound data (Fig. 8.1). The quality of the data is best along the seismic profiles, because the ship speed of ~6 knots during seismic profiling results in a better lateral resolution and a reduced noise level. However based on the steep morphology less information are available along the continental slope and the flanks of the Agulhas Plateau and Mozambique Ridge.

Profile AWI-20050100

PARASOUND profile on the position of the refraction seismic line AWI-20050100 extends from the shelf area offshore Mossel Bay to the Agulhas Plateau approximately North-South striking. Topography and sedimentation pattern change continuously along the profile. Different structures, e.g. channels, erosional surfaces, and areas of sediment accumulation are observed.

Water depth on the shelf is approximately 110m (Fig. 8.2). The sea floor reflects a uniform structure. Sediment input, e.g. by rivers and currents, is mostly transported to the upper slope. However, sediment lenses can be observed (Fig. 8.2). These extend laterally about 4 km with a mean thickness of approximately 5m and 2km with 2m high respectively. Furthermore, sediment basement shows significant internal structure of seaward dipping layers. These layers are nearly parallel in the northern part of the profile compared to the tilted layers in the south. Here dip angles changes along upper part of the profile.

A channel-like structure is monitored at 22 km (Fig. 8.2; mark 3) which indicates active erosion. Number of channel systems increase along profile AWI-20050100 further south.

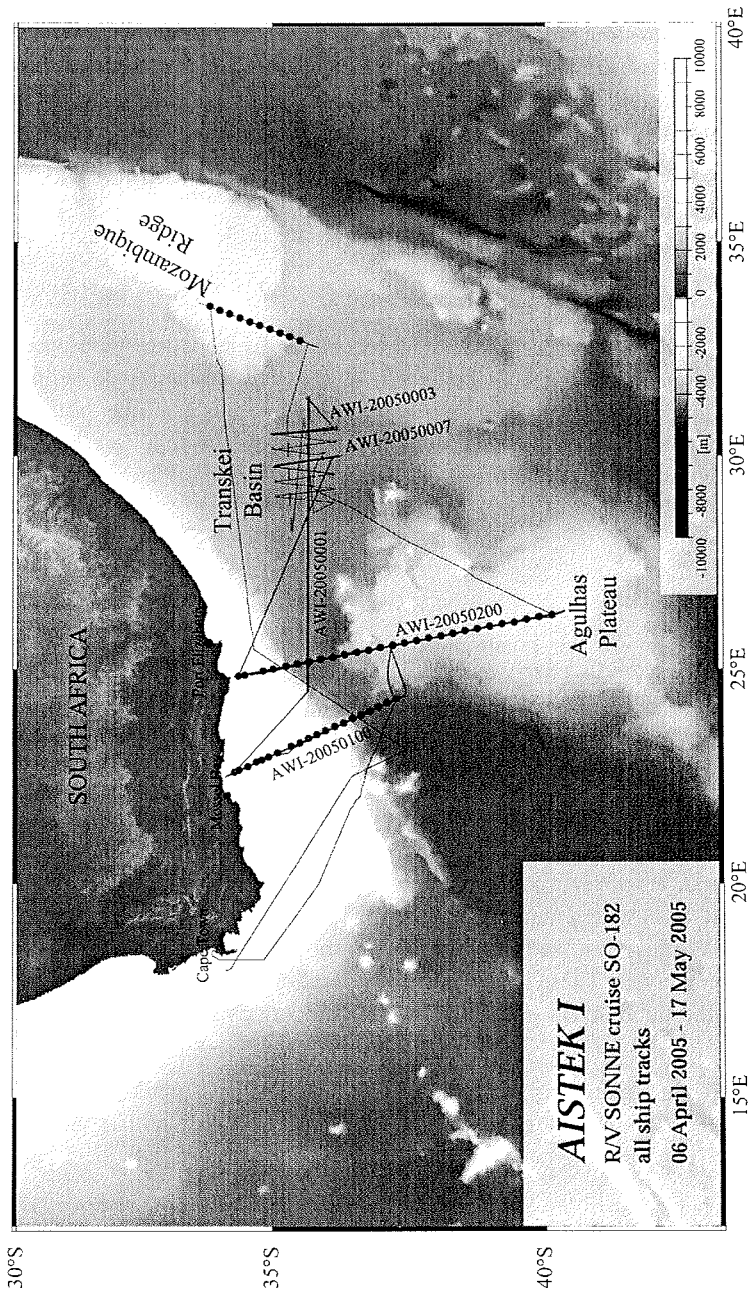


Fig. 8.1: Shown are all ship tracks recorded during SO-182; thick lines mark the profiles which are discussed in this chapter. GEBCO bathymetry is used.

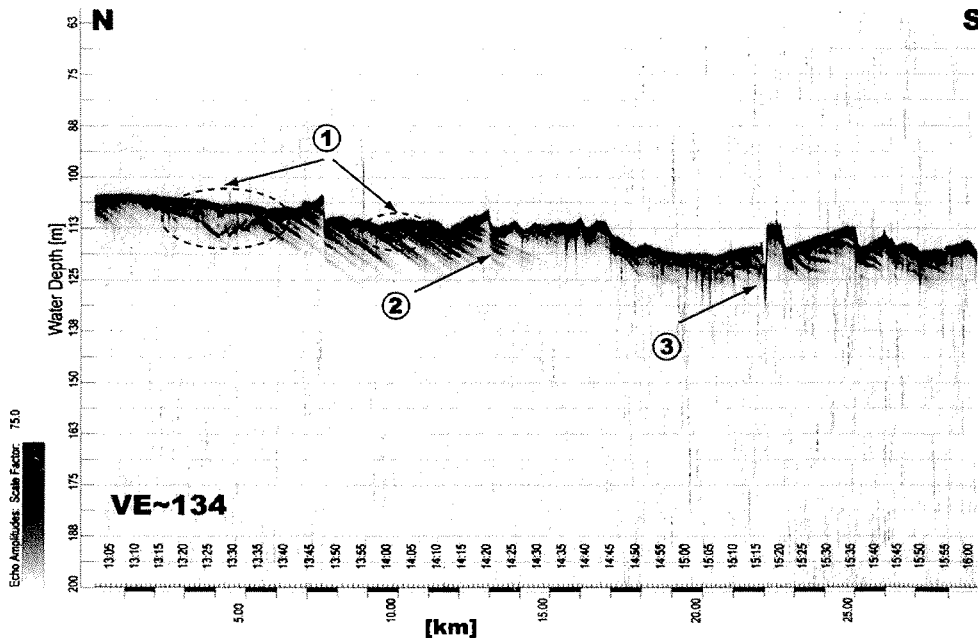


Fig. 8.2: Shown is the shelf area of profile AWI-20050100; (1) marks the position of sediment lenses. Tilted sediment basement (2) and erosional channel can be observed (3).

The PARASOUND profile from the deeper part of the Agulhas Passage illustrates increasing sedimentation rate along the profile from north to south (Fig. 8.3). At a depth of 4800m a strong reflector marks the base of a huge sediment body. This sediment accumulation extends from 2.5 -10km with an increasing thickness. Sediment sliding occurs at several steeper parts on top of this structure where the uppermost sediments are transported downhill. Southern-end of the profile is characterized by wavy pattern caused by large sediment accumulation.

Further south several channel systems determine the seafloor morphology (Fig. 8.4). Strong northward dipping reflectors indicate the formation of these channels by sliding of large blocks. The potential slide plains may indicate a major mass wasting process. Thus, these channels seem to be formed above the slide plains. A channel which is located at 4100m depth is filled with sediments whereas an identical structure at shallower water depth of 3700m shows no sediments. These features are also observed on profile AWI-20050200 where channels are filled at deeper water levels of 4000 – 4200m. In contrast channels in shallower water depth of less than 3800m accumulate no sediments indicating active erosion. Therefore, channel filling can be identified as an indicator for changes in water flow rates at different water depths.

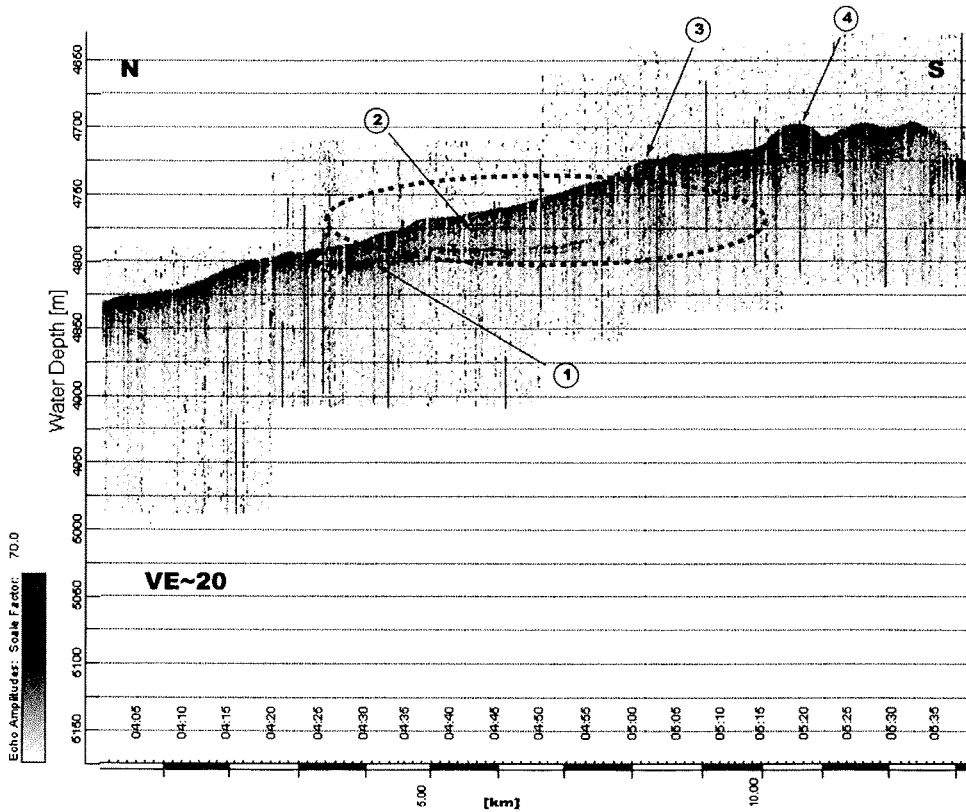


Fig. 8.3: A strong reflector (1) marks the base of a large sediment accumulation (2). Gravitational mass flow events (3) and wavy sediment pattern (4) are monitored on top of this sediment body.

In addition, a flat terrace, which is covered by layered sediments, is monitored at 3800m to 3900m. Internal layered structure of this sediment package gives evidence of a continuously undisturbed sedimentation.

Profile AWI-20050200

Nearly parallel east of profile AWI-20050100 a second PARASOUND profile AWI-20050200 was recorded. This profile starts also on the shelf offshore Mossel Bay but extends further south on top of the Agulhas plateau (Fig. 8.1). On the northern part of AWI-20050200 structures similar to profile AWI-20050100 are observed, e.g. a rough shelf with less sediment cover and an increase of sediment accumulation towards the Agulhas passage. Thus, examples from the Agulhas plateau are taken in this capture.

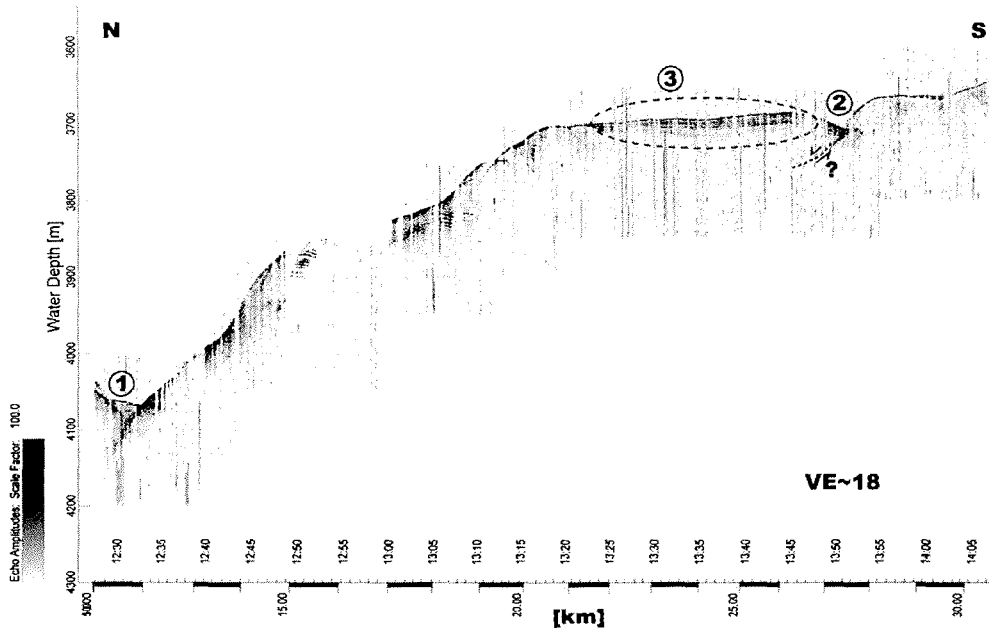


Fig. 8.4: This profile shows locations of channel systems (1, 2) and a flat terrace (3).

The northern flank of the Agulhas plateau is characterized by a steep and rough topography (Fig. 8.5). A mean slope angle of 3.2° with a steep upper slope of 5.7° and a lower slope angle of 2.7° are measured. Rough topography at the lower slope can be described as depositions caused by gravitational mass wasting. Furthermore, low penetration into the underground indicates a dense material with less sediment coverage along the upper slope. All sediments are eroded and transported to the lower slope as well as to the Agulhas passage. The northern end of the Agulhas plateau itself is marked by a single topographic high. This outcrop has a lateral dimension of 10km with an elevation of 150m above the plateau which follows to the south. Here an increasing sediment thickness is recorded.

The plateau topography varies in morphology (Fig. 8.6). The northern plateau recorded during this cruise shows a rough topography where no sediments are deposited. This rough seafloor indicates strong erosion processes, seen clearly at the steep eroded flanks as well as the V-shaped canyons where currents take away materials.

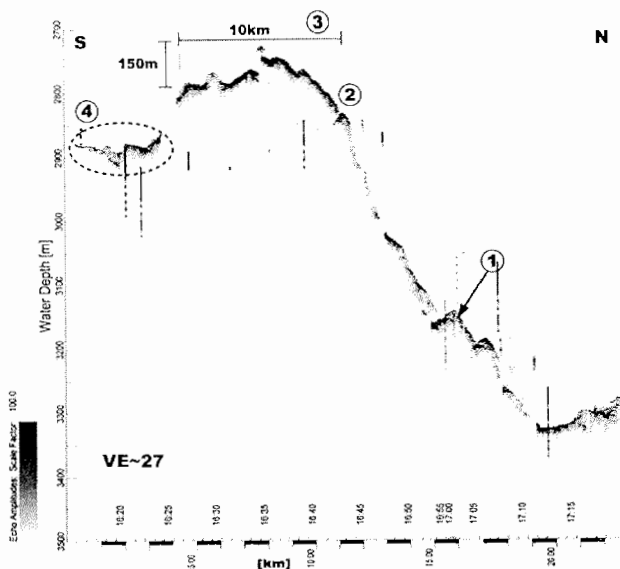


Fig. 8.5: Lower slope area is characterized by a rough topography (1). In contrast upper slope show no sediment cover and a steeper slope angle (2). Single outcrop marks northern end of Agulhas Plateau (3). Sediment cover increases on top of the Agulhas plateau along this profile (4).

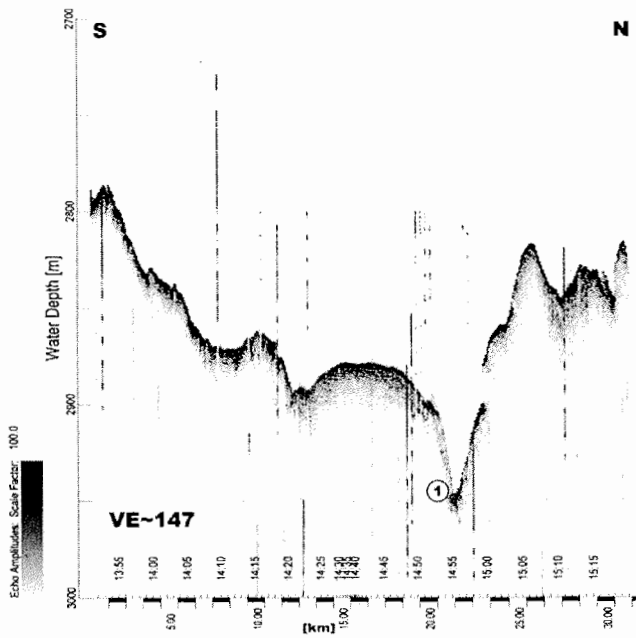


Fig. 8.6: This profile shows the rough topography of the Agulhas Plateau including a large channel system as a characteristic feature (1).

Profile AWI-20050001

PARASOUND data were also recorded along the EW - striking reflection seismic profile AWI-20050001 (Fig. 8.1).

The entire profile shows a closed sediment cover (Fig 8.7). Sediment penetration of up to 100m enables excellent data quality along the entire profile. Seafloor is characterized by a smooth topography where no highs or rough structures can be observed. In addition, no internal deformations are observed along the profile showing always a well-stratified sediment package (Fig. 8.7). Unfortunately no sediment cores exist which can be correlated with these data.

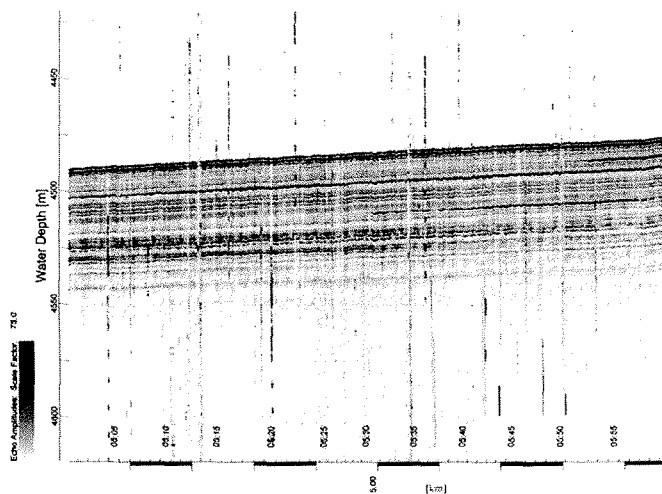


Fig. 8.7: PARASOUND profile recorded along reflection seismic line AWI-20050001.

Profiles AWI-20050003; AWI-20050007

Nearly perpendicular to AWI-20050001 several PARASOUND profiles were recorded. Similar to the EW striking line these data are characterized by an excellent penetration into sediments of up to 100m depth. Along all profiles no basement structures were observed.

On the easternmost profile AWI-20050003 a large sediment body was recorded (Fig. 8.8). This sediment accumulation has a lateral extension of approximately 23 km with a mean thickness of about 30m. The flat sediment basement where material is deposited can be well identified from PARASOUND data. Furthermore, the upper boundary of a highly transparent layer shows a wavy ripple-like surface. This indicates active currents and erosional behaviour.

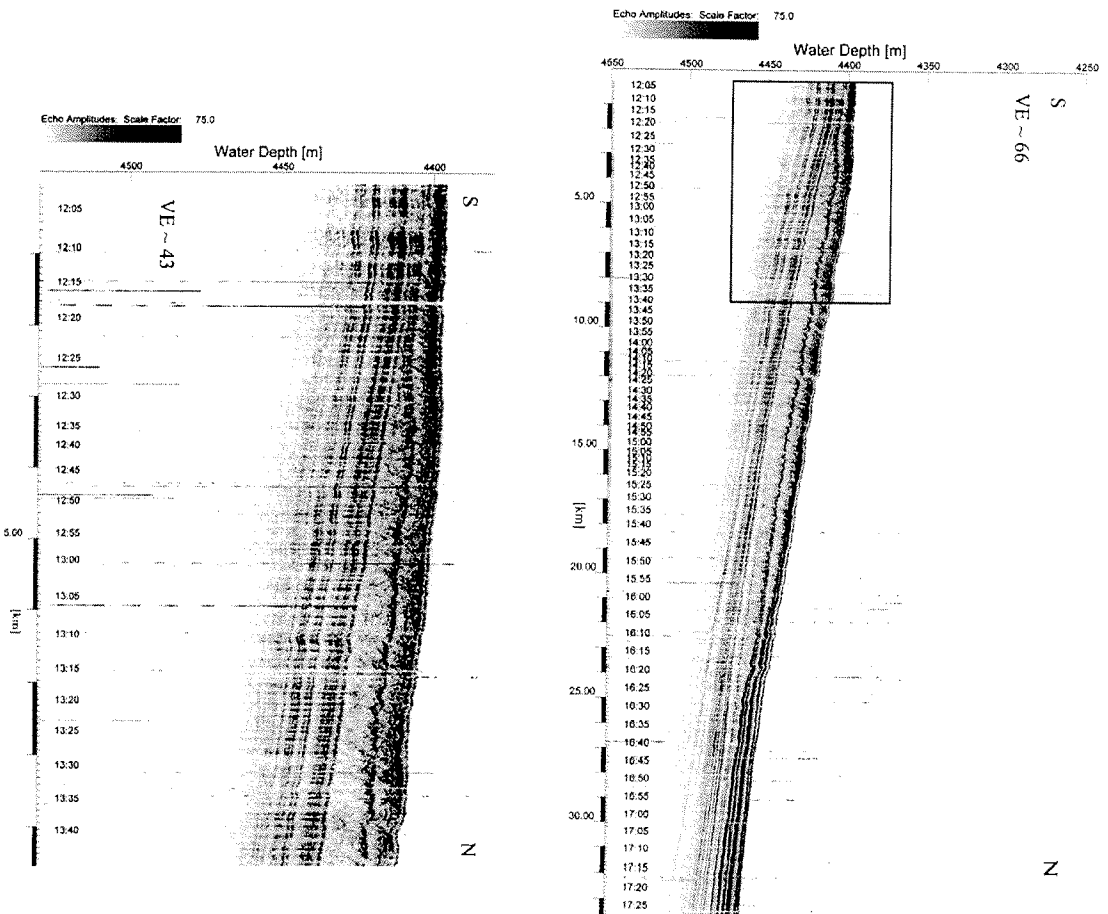


Fig. 8.8: Along profile AWI-20050003 a large sediment body could be observed. The upper figure shows the entire structure whereas only the southern part is seen in the lower figure.

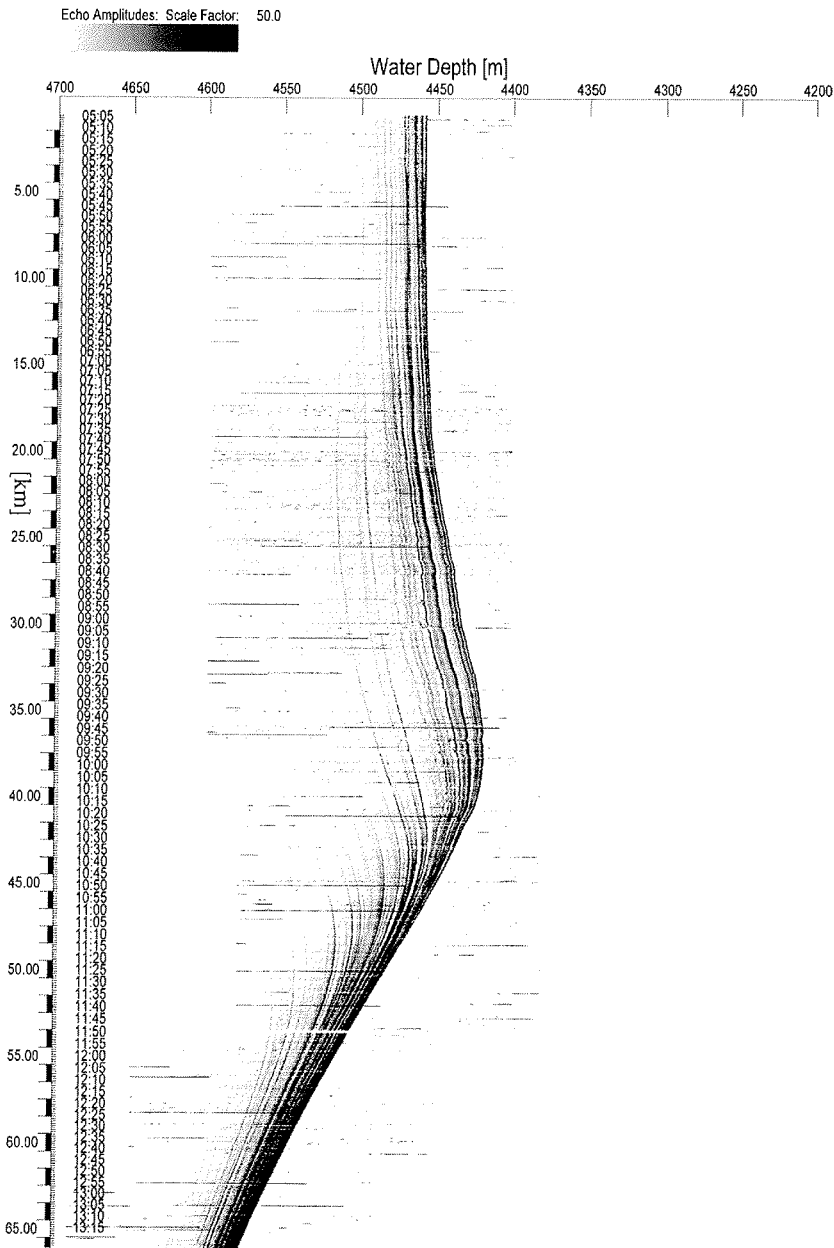


Fig. 8.9: Along profile AWI-20050007 a large sediment drift can be identified.

This sediment body builds up to a large sediment drift further west along profile AWI-20050007 which can also be observed along PARASOUND lines further west. A characteristic drift geometry is observed where a luff and respectively a lee side can be identified (Fig. 8.9). This structure extends about approximately 65 km with at least 100m thickness at the peak. In addition, internal structures enable investigation of the temporal as well as spatial evolution of this drift body.

In addition with reflection seismic data information from all NS striking profiles give a good opportunity to reconstruct the environmental as well as ocean circulation conditions during the drift growth.

9. Seismics

9.1 Methods

The application of seismic methods was the primary operational objective of SO-182 in order to obtain information on the deep structure and the seismic velocity distribution of the crust and the crust-mantle boundary of the Agulhas Transect and the sedimentary distribution of the Transkei Basin. (a) We used a standard multi-channel reflection seismic technique to image the outline and reflectivity characteristics of the sedimentary layers and the structure of the sub-sedimentary basement and lower crust by recording the returning near-vertical wave field. (b) Seismic refraction and wide-angle reflection techniques were used to obtain the distribution of seismic P- and S-wave velocity fields from recordings of large-offset and deeply penetrating refracted and reflected waves using ocean-bottom seismographs (OBS) and land-seismographs. Figure 9.1 illustrates the principles of both techniques.

9.2 Seismic equipment

9.2.1 Seismic sources, triggering and timing

(G. Uenzelmann-Neben, K. Gohl)

Several airgun source configurations were used, depending on target depths/distances and required resolution of the seismic data.

We used a cluster of 8 G-guns (520 inch³ each, 4160 inch³ = 66.56 l in total) deployed portside and a 32 l Bolt airgun deployed starboard side as the source for the seismic refraction profiles AWI-20050100, AWI-20050200 and AWI-20050300. The G-guns were separated by 2.3 m, and all guns were towed in a depth of 10m approximately 20 m behind the vessel (Fig. 9.2). The airguns were fired once per minute at 140 bar, leading to an average shot interval of 150 m.

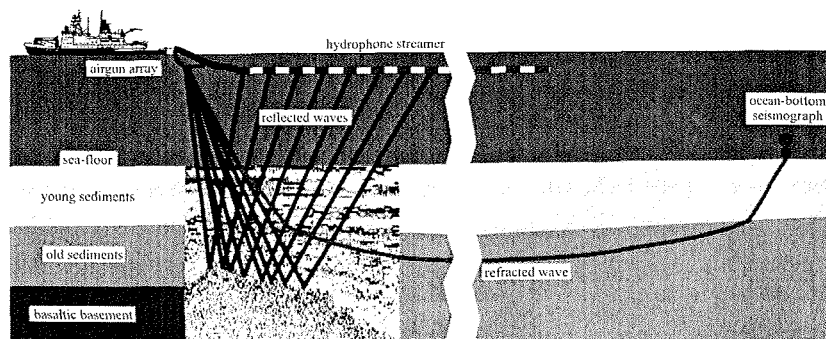


Fig. 9.1 Principles of marine seismic reflection and refraction surveying.

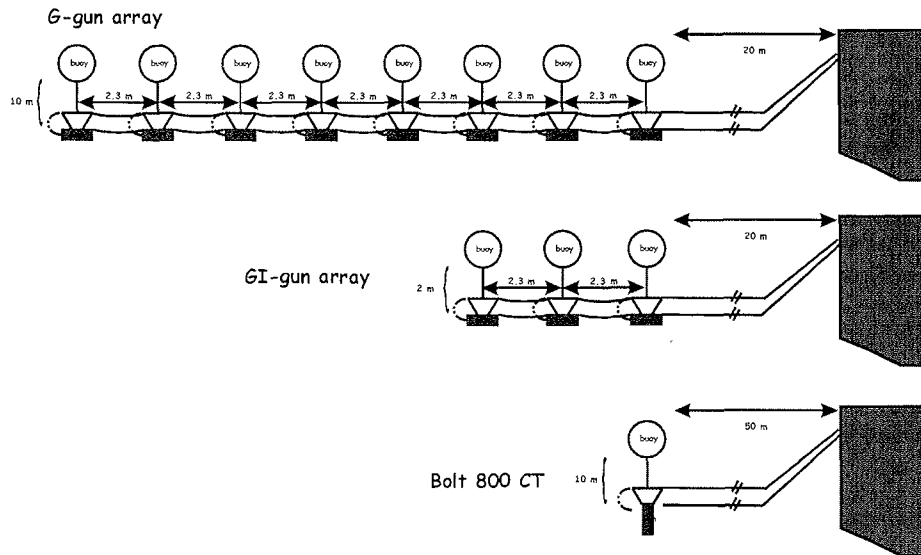


Fig. 9.2: Configuration of the different seismic sources used for seismic profiling.

The high resolution seismic reflection lines in Transkei Basin were shot using 3 GI-guns to better resolve the sedimentary layers (Fig. 9.2). A single GI-Gun™ is made of two independent airguns within the same body. The first airgun (“Generator”) produces the primary pulse, while the second airgun (“Injector”) is used to control the oscillation of the bubble produced by the “Generator”. We used the “Generator” with a volume of 0.72 litres (45 in³) and fired the “Injector” (1.68 litres = 105 in³) with a delay of 33 ms. This leads to an almost bubble-free signal. The guns were towed 20 m behind the vessel in 2 m depth and fired every 10 s (~25 m shot interval).

Seismic data acquisition requires a very precise timing system, because seismic sources and recordings systems must be synchronised. A combined electric trigger-clock system was in operation in order (1) to provide the firing signal for the electric airgun valves, (2) to provide the time-control of the seismic data recording and (3) to synchronise the internal clocks of the OBS/H systems. Due to the variable time difference in the NMEA format of the ship-provided clock and the DVS system, a separate Meinberg GPS clock was used with an antenna mounted on the upper deck. The clock provides UTC date and time minute and second pulses.

In accordance with the *Expanded Environmental Notification for Marine Geophysical Research off the South and South-East Coasts of South Africa* compiled by *CCA Environmental*, an independent observer constantly visually monitored the area in a radius of 3 km around the vessel for possible marine mammal appearance before and during seismic profiling. No marine mammals were detected before and during the seismic operations. Airguns were fired with gradually increasing working pressure (ramping up) at the beginning of a profile and after shot interruptions.

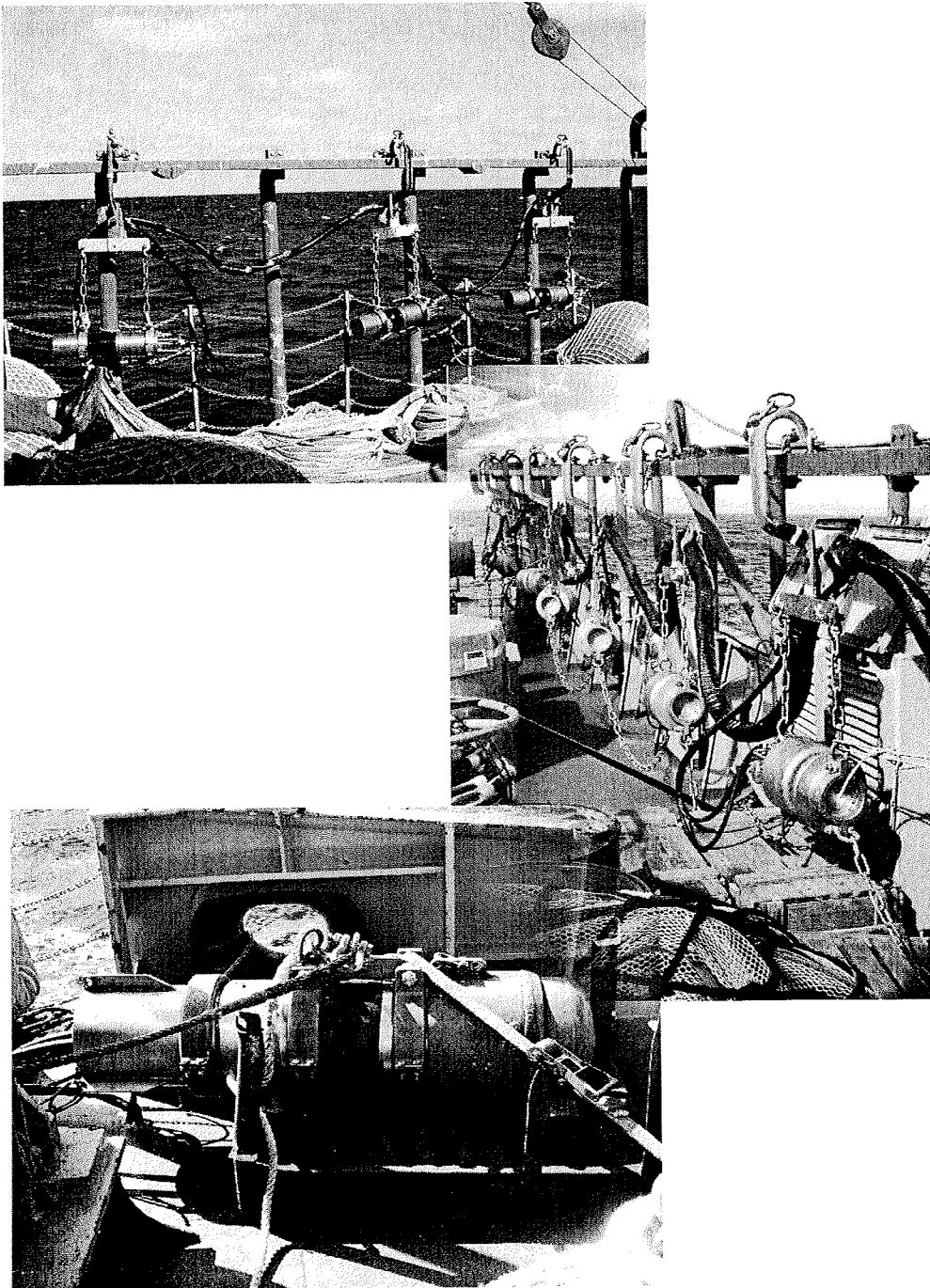


Fig. 9.3: The three different airgun configuration used during the cruise: 3 GI-guns (above), 8 G-guns (middle), and the 321 Bolt airgun (below).

9.2.2 Ocean-bottom seismometer/hydrophone systems (OBS/OBH)

(K. Gohl, E. Labahn, Ch. Nettling, J. Grobys, N. Parsiegla, D. Berger, A. Fahl)

Three types of OBS/H systems by IFM-GEOMAR were on board during SO-182, serviced mainly by K.U.M. Umwelt- und Meerestechnik Kiel GmbH: 14 OBS "3-foot", 15 OBS "flat" and 11 OBH systems. With the exception of one station on profile AWI-20050200 where an OBH (hydrophone only) was deployed, all stations were occupied with OBS systems with a hydrophone and a three-component seismometer each. Deployment and recovery coordinates and dates/times of the three OBS profiles are listed in Appendix II, IV, and VI.

- (1) The OBH system has its components mounted on a single beam steel rack (Fig. 9.4). Beneath a ring for deployment and retrieval purposes, the steel construction holds a floating body consisting of syntactic foam and a pressure chamber holding the acoustic releaser, pressure cylinder with seismic recording unit and power supply, hydrophone, flasher, radio beacon and flag. An anchor is suspended by a rope about 2 m below the rack.
- (2) One type of the OBS systems has its components mounted on a tripod steel rack (here named "OBS 3-foot") (Fig. 9.4) with the central steel rack holding a floating body consisting of syntactic foam and a pressure chamber holding the acoustic releaser, pressure cylinder with seismic recording unit and power supply, hydrophone, flasher, radio beacon and flag. The tripod sits directly on the anchor frame. From a 1.5 m long horizontally placed extension arm, the seismometers is suspended and dropped to the seafloor after an electrolytic wire has been dissolved from seawater after the systems touches the seafloor.
- (3) The more recent development of the IFM-GEOMAR OBS systems consists of a steel frame holding the acoustic releaser, pressure cylinder with seismic recording unit and power supply, hydrophone, flasher, radio beacon and flag as well as four cylindrical floating bodies of syntactic foam. The steel frame is mounted horizontally on an anchor frame (Fig. 9.5) and. In this "OBS flat" system, the seismometer is placed directly onto the anchor frame. On the first profile, a few systems had the seismometer suspended and dropped from an extension rod. These systems were thereafter modified to an anchor-attached position. When the OBS system is released from its anchor and floats back to the surface, it rotates into an upright position with the flasher, radio beacon and flag on top.

Two acoustic/time release units were used: (1) OCEANO (types RT-661 and RT-861) and (2) KUMQUAT type K/MT 562. The OCEANO acoustic release communicated with an OCEANO Telecommand deck unit (model TT-300 B), the KUMQUAT releaser communicated with deck unit EdgeTech 8011A. Both deck units were connected to the hydrophone installed at the bottom of the hull ("Spargel") and operated from the bridge. All acoustic releasers were tested to 4000 m water depth, mounted on the rosette frame in conjunction with two CTD instruments for Simrad calibration. It is noted that acoustic responses such as ranging and diagnostics from either type of releaser could not be registered, unless the systems were close to the sea surface. This observation was made not only for the releaser test but for regular OBS deployment/retrieval of all three profiles as well. However, the anchor release functions worked properly.

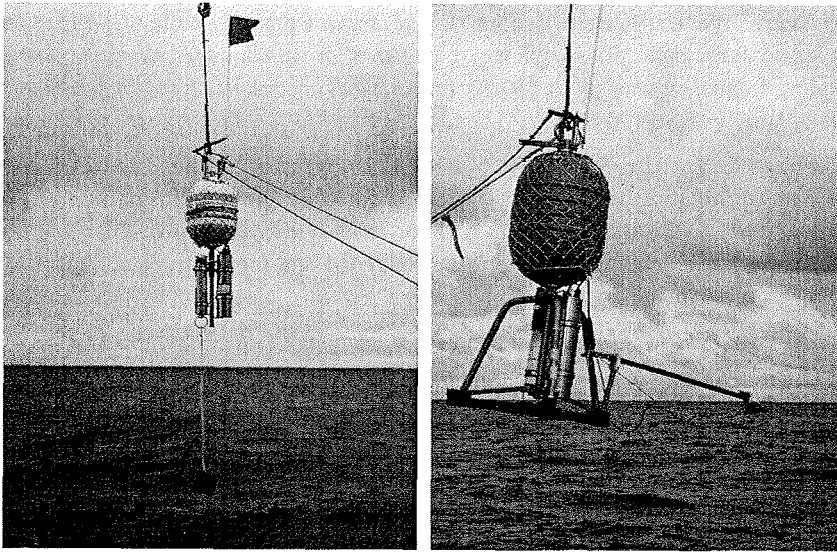


Fig. 9.4: IFM-GEOMAR OBH system (left) and OBS 3-foot (right) before deployment.

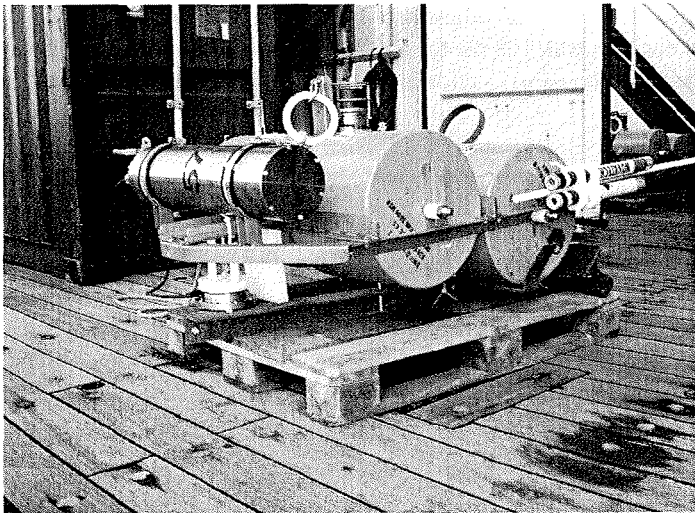


Fig. 9.5: IFM-GEOMAR OBS flat system before deployment.

All OBS/OBH systems operated with the seismic hydrophone type E-2PD made by OAS Inc. The seismometers were of type Owen with a natural frequency of 4.5 Hz. On profile AWI-20050200, we had to use a few seismometers with a natural frequency of 15 Hz. Xenon flashers and radio beacons (channels C and D) were of NOVATECH type.

Two types of seismic recorders were used, both manufactured by SEND GmbH:

- (1) The Marine Broadband Seismocorder (Methusalem-MBS) stores the data on up to four IBM-MicroDrives or flash cards via PCMCIA sockets. The pre-amplified analogue input signal is digitized by a 16-bit signed sigma-delta A/D converter. 1 GB

IBM-MicroDrive Cards were used for storage. From a possible scale of 1-31, the gain was set to 5 for hydrophone channel 1 and to 9 for seismometer channels 2-4. The sampling frequency was set to 250 Hz for all MBS recorders, except one which was unintentionally set to 125 Hz.

- (2) The Marine Exploration Seismocorder (GEOLON-MES) writes the data to an internal hard disk of 30 GB space. The pre-amplified analogue input signal is digitized by a high-performance 24-bit sigma-delta A/D converter. From a power-of-2-scale of 1-64, the gain was set to 16 for the hydrophone channel 1 and the seismometer channels 2-4. The sampling frequency was set to 250 Hz.

Both recorder types are powered by a rechargeable lead-acid battery or a block of multiple 1.5-V-monocells to provide 12 V. A number of rechargeable batteries proved to be unreliable on the first profile, as they dropped their voltage to 8.0-10 V after instrument retrieval. One instrument stopped recording prematurely due to the battery failure. Therefore, only monocells were used for the subsequent profiles.

The recording parameters were set via the PC control program SENDCOM which also controls the time synchronisation of the internal clock with the external GPS clock. On this survey, we used a Meinberg GPS-166 clock for synchronization which also provided the airgun trigger pulse. Therefore, no adjustment for time-shift between clocks had to be made. The maximum skew time was 108 ms for a 4-day + 4-hour recording. The parameter setting and the skew time for each OBS/H station are listed in Appendices II, IV, and VI.

9.2.3 Land-based seismic recorders and shots

(A. Schulze, K. Gohl)

The deep crustal seismic part of the Agulhas-Karoo Geoscience Transect on the mainland with a landward extension of the two OBS profiles AWI-20050100 and 20050200 was conducted by the GeoForschungsZentrum Potsdam. The western line is situated between Fraserburg and Heroldsbay; and the eastern line extends from Graaf Reinet to Cape St. Francis (south of Humansdorp) (Figs. 1.1 and 9.7).

The western line has a length of about 240 km with 48 seismic receivers deployed. 45 seismic receivers were installed along the eastern line which is about 225 km in length. Average receiver spacing is therefore 5 km. Every receiver station consisted of a 3-component 4.5-Hz geophone and an EarthData Logger which sampled at 100 Hz. A 38-Ah battery was used as power supply sufficient for a time span of five to six days (including deployment and recovery). The time base was provided by GPS.

Thirteen explosive shots were fired for each line with an average spacing of about 20 km (coordinates and charge sizes are given in Appendices III and V). In order to achieve a better source signal, each shot point consisted of two holes.

9.2.4 Multi-channel reflection recording system

(S.Sibthorp, K. Coldham)

For multi-channel reflection data acquisition, a complete digital seismic streamer and recording system was provided by Exploration Electronics Ltd. (UK) as contractor to AWI. The system consists of a large capacity, fully integrated, high resolution marine seismic data acquisition system (SERCEL SEAL™) which is composed of both onboard and in-sea equipment (Fig. 9.6). The streamer is a 180-channel hydrophone array which is coupled to the onboard recorder via a fibre-optic tow leader and a deck lead. The data collected by the hydrophone array is firstly converted from an analogue signal to digital via an A/D converter and then converted to a 24-bit complement format at 0.25 ms sample rate by a DSP. The data is routed to a Line Acquisition Unit Marine (LAUM) at this point, one of these being located every five Acquisition Line Sections or 750 m. The LAUM decimates, filters and compresses the data before routing them through the tow leader and deck lead to the on-board equipment.

The coupling of the streamer with the Control Module (CMXL) is made via the Deck Cable Crossing Unit (DCXU) which also acts as a LAUM for the first 60 channels of the streamer. The CMXL decompresses, demultiplexes and then performs IEEE 32-bit conversion to the data. The data are collected via a network switch and converted to SEG-D by the PRM, the PRM being a processor software module used for formatting data to and from the cartridge drives, the plotters and Seapro QC™.

All system parameters can be set through the Human Computer Interface (HCI) which displays the systems activity such as print parameters, log files, high resolution graphic display and test results.

Cable depth keeping was monitored on Digicourse™ software, and adjustment to depths was made with Digibirds™, Model 5010. The Digicourse™ software gives a continuously updated graphical display of depths and wing angles via the Digibirds™ which are situated at 300 m intervals along the streamer.

<i>Acquisition Line Section Spec.</i>	
Length	150 m
Channels	12
Phones/group	16
Group length	12.5 m
Sensitivity	20 V/Bar open ended
Capacity	256 µf

The data were recorded with the following parameters (also Appendix I):

<i>Profile Name</i>	<i>Active Length</i>	<i>Lead-in</i>	<i>Record Length</i>	<i>Sample Rate</i>
AWI-20050001	2250 m	150 m	9 s	1 ms
AWI-20050002	2250 m	170 m	9 s	1 ms
AWI-20050003	2250 m	170 m	9 s	1 ms
AWI-20050004	2250 m	170 m	9 s	1 ms
AWI-20050005	2250 m	170 m	9 s	1 ms

AWI-20050006	2250 m	170 m	9 s	1 ms
AWI-20050007	2250 m	170 m	9 s	1 ms
AWI-20050008	2250 m	170 m	9 s	1 ms
AWI-20050009	2250 m	170 m	9 s	1 ms
AWI-20050010	2250 m	170 m	9 s	1 ms
AWI-20050011	2250 m	170 m	9 s	1 ms
AWI-20050012	2250 m	170 m	9 s	1 ms
AWI-20050013	2250 m	170 m	9 s	1 ms
AWI-20050014	2250 m	170 m	9 s	1 ms
AWI-20050015	2250 m	170 m	9 s	1 ms
AWI-20050016	2250 m	170 m	9 s	1 ms
AWI-20050017	2250 m	170 m	9 s	1 ms
AWI-20050018	2250 m	170 m	9 s	1 ms
AWI-20050100	2250 m	150 m	15 s	2 ms
AWI-20050200	2250 m	170 m	15 s	2 ms
AWI-20050300	2250 m	170 m	15 s	2 ms

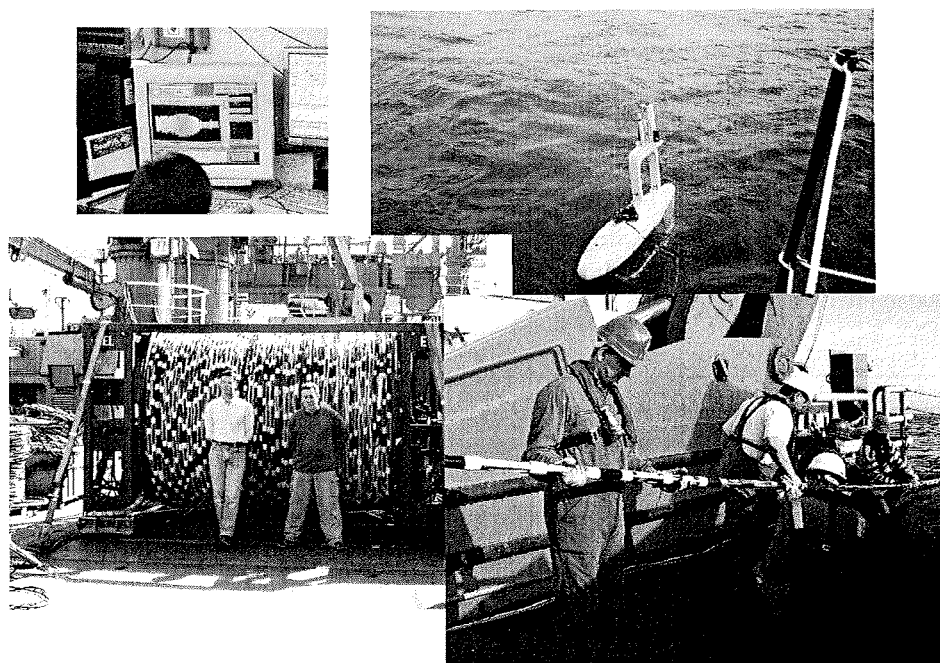


Fig. 9.6: SERCEL SEAL™ digital multichannel seismic system, provided by Exploration Electronics Ltd., and the recordings units.

9.3 Processing of multi-channel reflection data

(G. Uenzelmann-Neben)

As soon as the seismic reflection lines were gathered standard processing of the data was supposed to start. Unfortunately, due to irresolvable problems with a tape drive and a disk we could only read in the data for a quick quality check and the generation of a constant-offset-plot. This was carried out on a SGI Origin 200™ supercomputer using the FOCUS™ processing software. A band pass filter was applied for the plot.

9.4 Preliminary results of multi-channel reflection data

(G. Uenzelmann-Neben, P. Schlüter, G. Eagles, A. Gebauer, C. Gebhardt, S. Schneider, E. Weigelt)

As detailed seismic processing is time-consuming and could not be carried out on board, only a first, preliminary interpretation could be performed on board during the cruise.

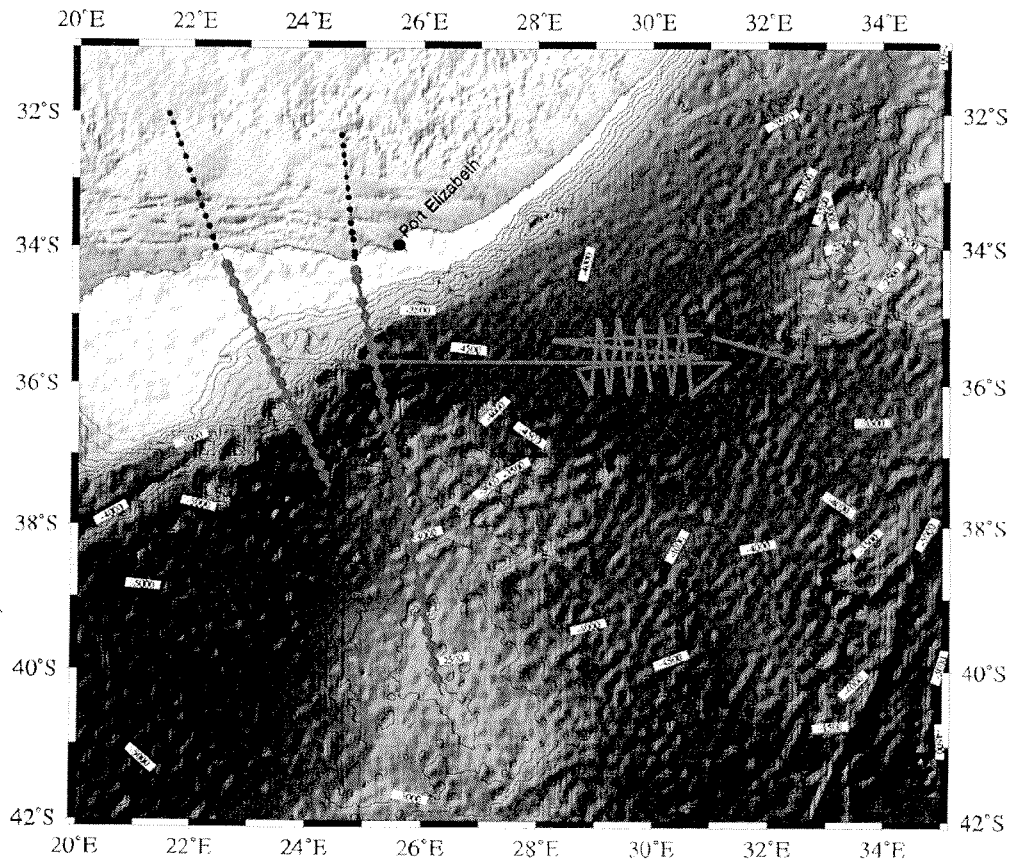


Fig. 9.7: Satellite derived topography (Smith and Sandwell, 1997) of the area of investigation showing the seismic lines acquired during this cruise in red. Red dots refer to the locations of the ocean bottom seismometers, and black dots to the locations of the land shots.

9.4.1 The Agulhas Transect

The Agulhas Transect consists of seismic profiles acquired from the continental shelf across the Outeniqua Basin and the Agulhas Passage onto the Agulhas Plateau (Fig. 9.7). The shelf is characterised by subparallel reflectors, which have been eroded both on the shelf and the slope. The Outeniqua Basin is filled with more than 2 s TWT thick well layered sediments. These sequences can be traced onto the shelf. Towards the SE the sedimentary layers rise and thin onto the Diaz Ridge. A number of internal reflections can be identified on the Diaz Ridge, which at this stage of processing are difficult to correlate.

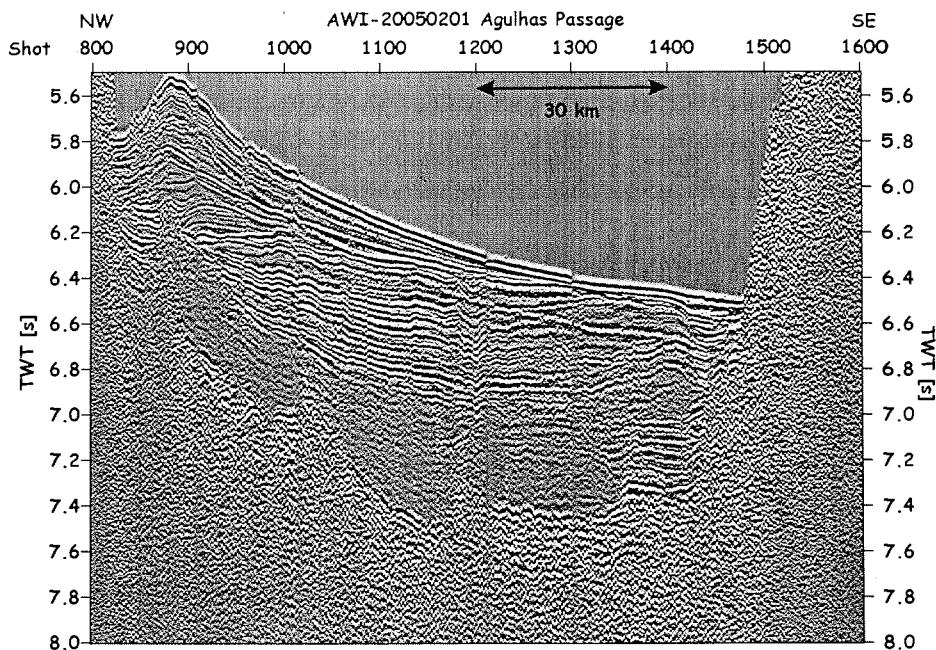


Fig 9.8: Part of line AWI-20050201 showing the Agulhas Passage. Note the sediment drift located in the northern part of the passage. This is a Constant-Offset plot without any gain applied.

The Agulhas Passage is characterised by a varying sedimentary cover. In places the sequences are quite thin, whereas elsewhere we observe sediment drifts, which are up to 1.25 s TWT thick (Fig. 20050201_800). This is most probably due to the influence of oceanic currents. The transition to The Agulhas Plateau is very steep, and little sediment can be found on the northern Agulhas Plateau. We observe only small basin with up to 400 ms thick sediments between basement high. Only south of $39^{\circ}10'$ the sedimentary thickness increases (Fig. 20050201_3500). We have identified lava flows originating at the basement highs, which document the volcanic history of the northern Agulhas Plateau.

9.4.2 The Transkei Basin

The western Transkei Basin shows flat seismic reflectors indicating constant, continuing sedimentary conditions. We can distinguish four sedimentary horizons, which may be

correlated with the seismostratigraphic models defined by Tucholke and Embley (1984) and Niemi et al. (2000). These horizons probably represent major changes in the current and thus sedimentary regime. Especially the deepest of the four reflectors is affected by erosion.

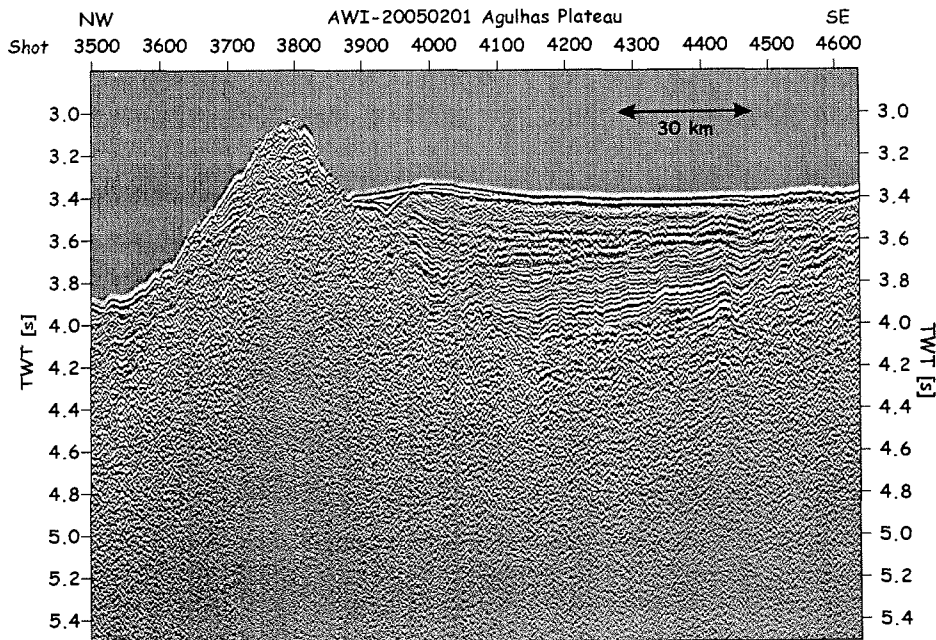


Fig. 9.9: Part of line AWI-20050201 showing a basement high a sedimentary basin on the central Agulhas Plateau. This is a Constant-Offset plot with no gain applied.

Additionally, the top of basement can be identified as a prominent reflector. In general, the basement is smooth. At $\sim 26^{\circ}\text{E}$ we observe a basement high, which rises up to the seafloor. Here, the sedimentary reflectors show onlap indicating a pre-sedimentary origin for the basement high.

In the southeastern part of the Transkei Basin the basement is quite rough. Here, we observe up to 1.6 s TWT thick sediments. The upper 200 ms TWT are characterised by contouritic structures. West of $30^{\circ} 30'\text{E}$ we identified the Agulhas Drift. It builds up from a ~ 20 ms TWT thick sedimentary lense in the east to a 420 ms TWT thick drift in the west. The base is formed by a reflector, which was defined as Pliocene by Niemi et al. (2000). The steeper flank can be found in the south, while the northern flank is rather flat (Fig 20050010). The topography of the drift becomes more pronounced when moving westwards. Furthermore, the crest moves towards the north on the western lines. This axis of the Agulhas Drift runs in N-S direction from which we conclude that the drift was built-up by an E-W setting current.

The base of the Agulhas Drift is inclined towards the south, and the drift shows onlaps onto this surface. We observe a strong change in reflection characteristics from below this surface (few internal reflections) to above (high reflectivity). The E-W profiles revealed that this surface forms the top of an old sediment drift with a W-E axis (Fig.). The crest of the drift lies in the east. The sequences of the drift show downlaps onto its base. Thus, this sediment drift

was built-up by a N-S setting current. We hence observe a major reorganisation of the current system in Pliocene times.

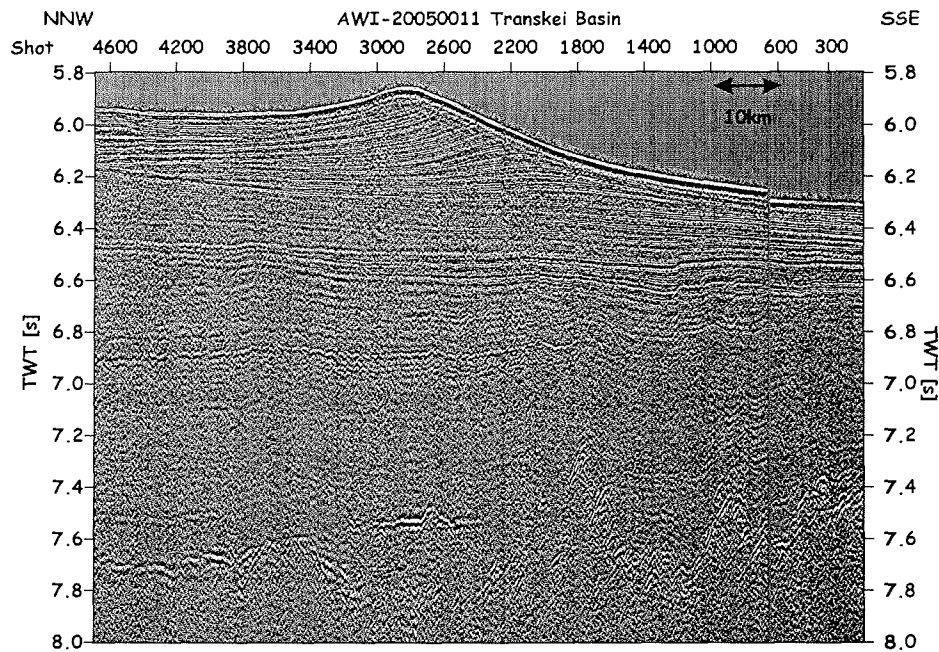


Fig. 9.10: Line AWI-20050010 showing the Agulhas Drift. This is a Constant-Offset plot with no gain applied.

The basement underneath the Agulhas Drift shows a number of highs, which can be correlated across the whole area investigation. But those basement highs have no influence on the structure of the drift itself.

9.4.3 The Mozambique Ridge

The southern part of the Mozambique Ridge was covered by one high-resolution and one deeper seismic reflection profile. Both lines show a very steep rise from the Transkei Basin to the ridge. This rise is about 1.3 km high. In general, the Mozambique Ridge shows a rugged topography (Fig.). Basement highs up to 800 m high alternate with sedimentary structures, which show a thickness up to 500 m. In places, the sediments are less than 100 m thick.

At this stage of processing, little can be said about the origin of the sedimentary units. The features will be much better imaged after stacking and migration, and fault systems, which are not resolvable from the cof-plot, can then be mapped.

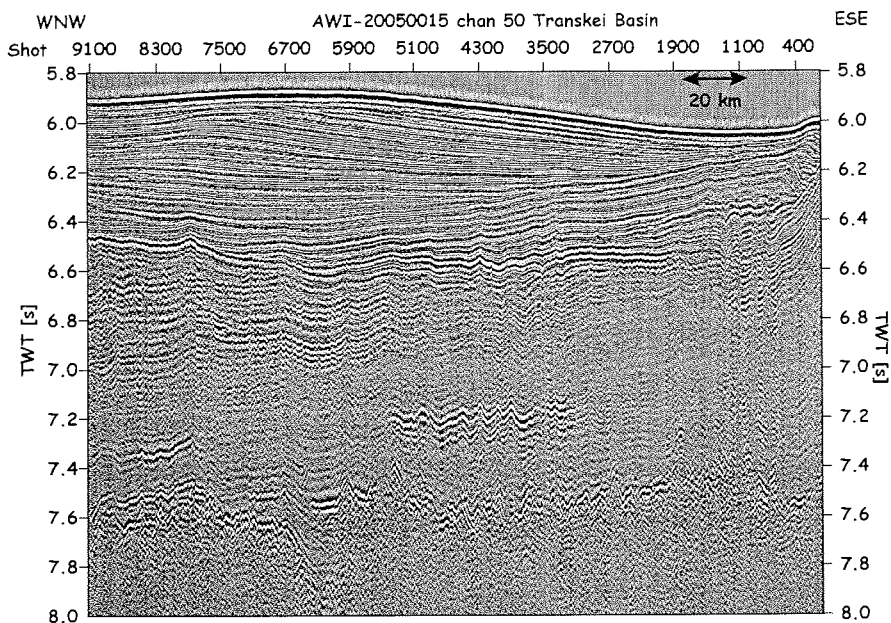


Fig. 9.11: W-E cross section across the Agulhas Drift showing an older sediment drift underneath. This is a Constant-Offset plot with no gain applied.

9.5 Processing of refraction/wide-angle OBS/OBH data

(K. Gohl, N. Parsieglä, J. Grobys, A. Fahl)

The OBS/OBH data acquired from the 57 stations were subject to onboard processing that consisted of the following steps:

- (1) The MBS and MES recorder were connected to the GPS clock and the PC running the SEND program *sendcom*.
- (2) Recording was ended and time skew was taken in order to obtain the time drift of the internal clock of the recorder compared to GPS time. This closes the PCMCIA card.
- (3) The MBS data and log files were downloaded (copied) from IBM-MicroDrives to a Windows PC. The MES records and log files were downloaded through a FireWire interface connection to a Linux PC using the *send2x* package commands *meslog* and *mescopy* (SEND GmbH).
- (4) The data files were pre-processed with the Linux version of the *send2x* program package (version 2.5). The routines *mbsread* or *mesread* extracts the data from the raw data files according to a given time window (shot time window). The routine *seg-ywrite* demultiplexes the data, adds shot and station coordinates to the trace headers and converts the data to SEG-Y format. The program requires a shot-point coordinate file. A SEG-Y file for every channel with trace lengths of 60 s was written, beginning at the exact shot time.
- (5) Using CWP/SU (SeismicUnix) software, the SEG-Y files were converted to SU

format and displayed for a first quality check.

- (6) The data were transferred to a Unix SGI computer for which we had a license to run the FOCUS™ processing software by Paradigm Ltd. After shot-receiver offset calculation, band-pass filtering (4-30 Hz), travel-time reduction and optimizing display parameters, the OBS/H records were displayed and printed for a first data analyses.

The final data processing with all necessary corrections will be performed with the FOCUS™ processing software at AWI. The onboard processing served primarily for data quality control.

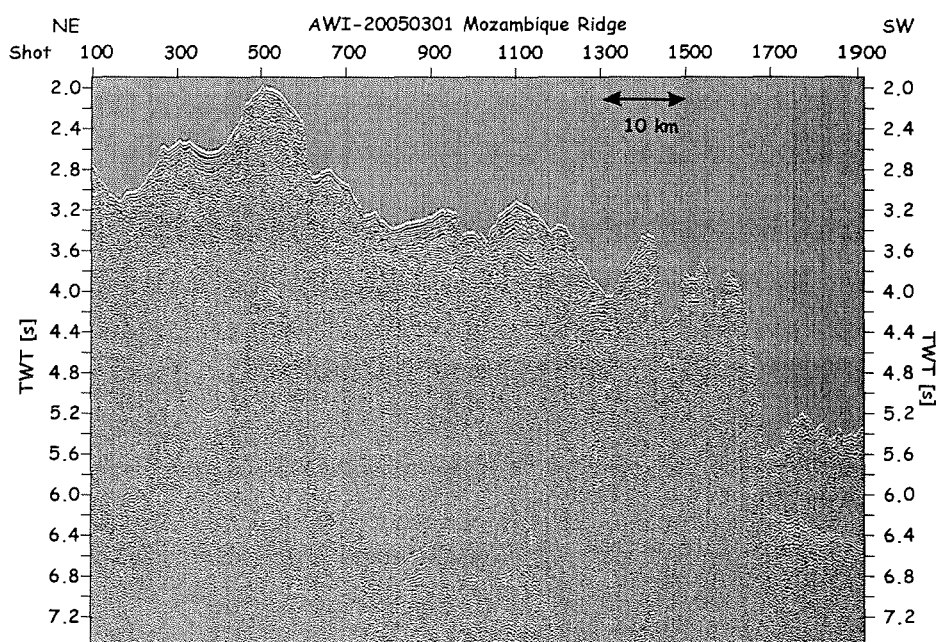


Fig. 9.12: Line AWI-20050301 from the Transkei Basin onto the Mozambique Ridge. This is a Constant-Offset plot with no gain applied.

9.6 Quality and preliminary results of refraction/wide-angle OBS data

(K. Gohl)

Of the 57 stations with OBS/H systems deployed along the three profile AWI-20050100, AWI-20050200 and AWI-20050300 (Fig. 9.7), three instruments failed to record data; one due to a burnt fuse, the other due to an error we could not track down, and the third did not record due to a human programming error. One recorder stopped recording before the end of shot profile AWI-20050100, probably due to power failure. The data of 4 instruments could not be read with the MBS/MESREAD routines and will have to be sent to SEND GmbH for recovery. All other instruments recorded mid- to highest-quality 3-component and/or hydrophone data from the airgun shot profiles (Appendices II, IV, and VI).

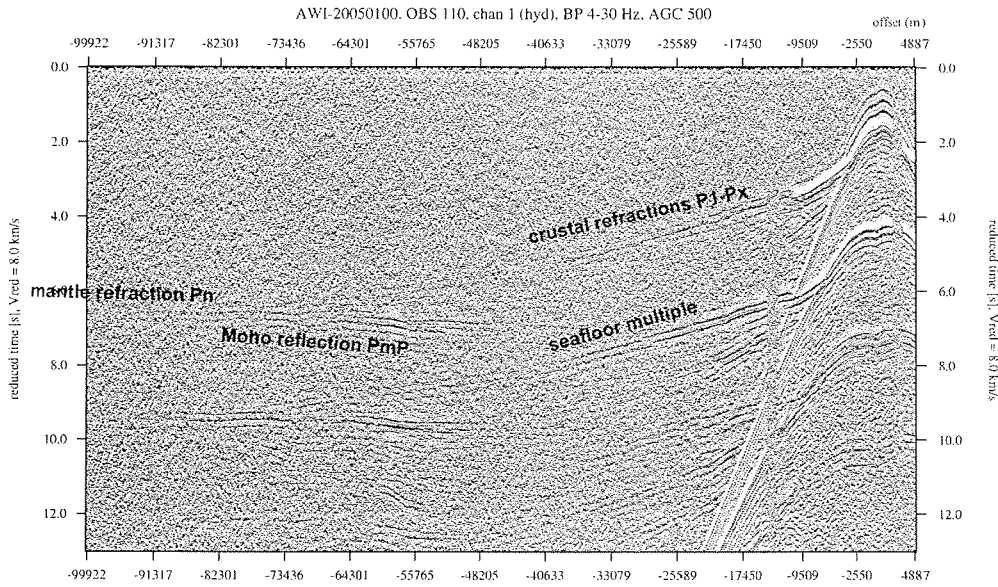


Fig. 9.13: Example of OBS data from line AWI-20050100, station 110 on the continental slope.

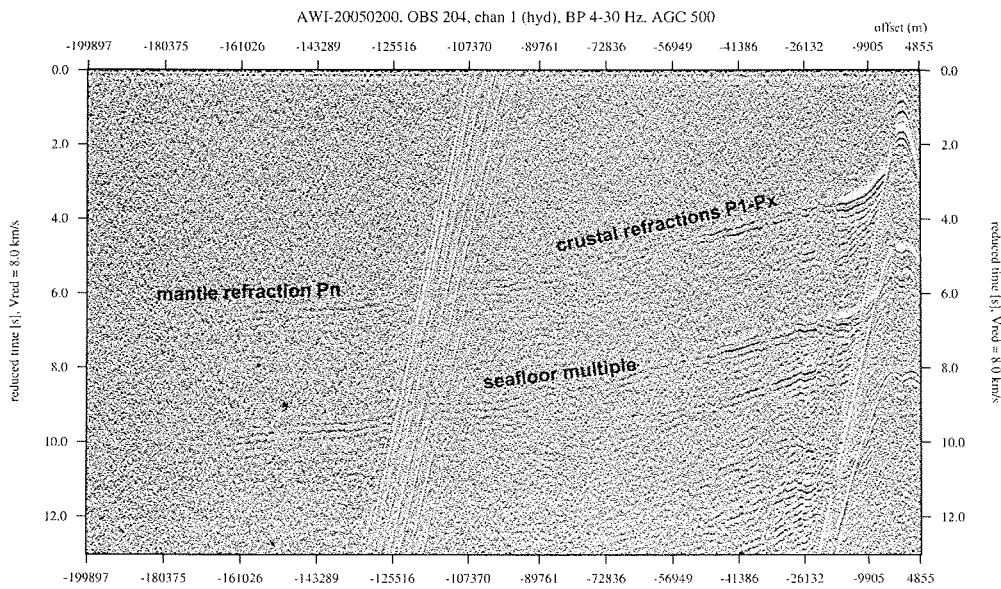


Fig. 9.14: Example of OBS data from line AWI-20050200, station 204 on the Agulhas Plateau.

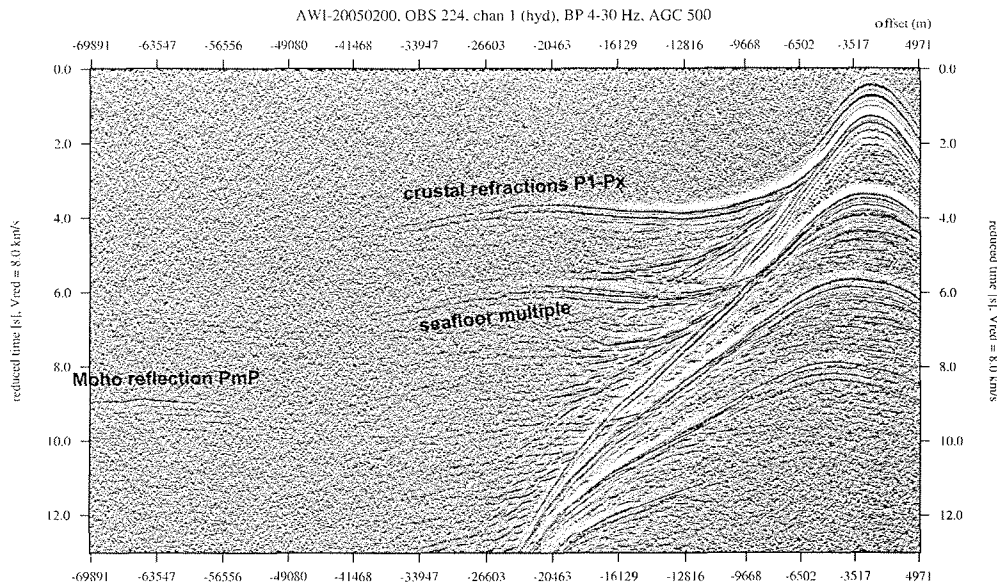


Fig. 9.15: Example of OBS data from line AWI-20050200, station 224 on the Agulhas Bank.

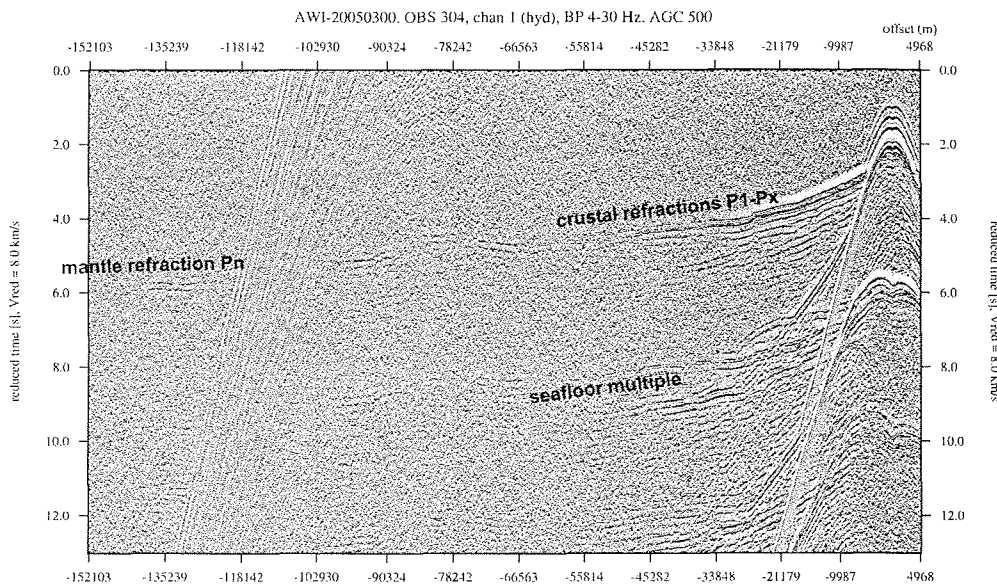


Fig. 9.16: Example for OBS data from line AWI-20050300, station 304 on the southern Mozambique Ridge.

Most records of excellent quality show P-wave arrivals of up to 200 km offset (data examples in Figs.9.13 – 9.16...). Refracted arrivals from the upper to lower crust (P_1 to P_x) are identified. S-wave arrivals are observed in most records but their offset range is mostly

limited to about 60-80 km. While mid-crustal wide-angle reflections appear sparse in most records, large-amplitude P_mP reflection phases from the crust-mantle boundary (Mohorovicic discontinuity) are easily identified. Refracted phases from the upper mantle (P_n) can be seen in most records which will allow an accurate model of variations in crustal thickness.

Due to the presumed large variation in structure and crustal thickness along this and the other profiles, we refrained from any preliminary 1-dimensional and, therefore, erroneous modelling approaches for this report. Decent velocity-depth modelling has to be performed in a full 2-D ray-tracing and travel-time inversion approach for which there was not enough time on board.

10. Acknowledgements

We wish to express our gratitude to the master L. Mallon and his officers and crew of RV "Sonne" for their professional and enthusiastic engagement and service to the scientific program of this leg. We are thankful to Maarten de Wit and George Smith from the University of Cape Town for their assistance in planning the cruise and Ian Mclachlan from the Petroleum Agency SA for helpful discussions. This cruise leg SO-182 and the project AISTEK-I are primarily funded by the German Federal Ministry of Education and Research (BMBF) under Project Number 03G0182A. Additional funding comes from the Alfred Wegener Institute.

11. References

- Allen, R.B.; Tucholke, B.E. (1981), Petrography and implications of continental rocks from the Agulhas Plateau, southwest Indian Ocean. *Geology*, 9, 463-468.
- Antoine, L.A.G.; Moyes, A.B. (1992), The Agulhas Magsat anomaly: implications for continental break-up of Gondwana. *Tectonophysics*, 212, 33-44.
- Ben-Avraham, Z.; Hartnady, C.J.H.; Malan, J.A. (1993), Early tectonic extension between the Agulhas Bank and the Falkland Plateau due to the rotation of the Lafonia microplate. *Earth and Planetary Science Letters*, 117, 43-58.
- Ben-Avraham, Z.; Hartnady, C.J.H.; le Roex, A.P. (1995), Neotectonic activity on continental fragments in the Southwest Indian Ocean: Agulhas Plateau and Mozambique Ridge. *J. Geophys. Res.* 100, 6199-6211.
- Ben-Avraham, Z.; Hartnady, C.J.H.; Kitchin, K.A. (1997), Structure and tectonics of the Agulhas-Falkland Fracture Zone. *Tectonophysics*, 282, 83-95.
- Ben-Avraham, Z.; Niemi, T.M.; Hartnady, C.J.H. (1994). Mid-Tertiary changes in deep ocean circulation patterns in the Natal Valley and Transkei Basin, Southwest Indian Ocean. *Earth and Planetary Science Letters*, 121, 639-646.
- Caress, D.W.; D.N. Chayes (1996), Improved processing of Hydrosweep DS multibeam data on the R/V Maurice Ewing. *Marine Geophysical. Research.* 18, 631-650.
- Camden-Smith, F.; Perrins, L.A.; Dingle, R.V.; Brundridt, G.B. (1981), A preliminary report on log-term bottom-current measurements and sediment transport/erosion in the Agulhas Passage, Southwest Indian Ocean. *Marine Geology*, 39, 81-88.
- Chetty, P.; Green, R.W.E. (1977), Seismic refraction observations in the Transkei Basin and adjacent areas. *Marine Geophys. Research*, 3, 197-208.
- Dingle, R.V.; Camden-Smith, F. (1979), Acoustic Stratigraphy and Current-Generated Bedforms in Deep Ocean Basins off Southeastern Africa. *Mar. Geol.* 33, 239-260.
- Dingle, R.V.; Birch, G.F.; Bremner, J.M., de Decker, R.H.; du Plessis, A.; Engelbrecht, J.C.; Fincham, M.J.; Fitton, T.; Flemming, B.W.; Gentle, R.I.; Goodlad, S.W.; Martin, A.K.; Mills, E.G.; Moir, G.J.; Parker, R.J.; Robson, R.H.; Simpson, E.E.W.; Summerhayes, C.P.; Westall, F.; Winter, A., and Woodborne, M.W. (1987), Deep-sea Sedimentary Environments Around Southern Africa (South-east Atlantic and South-west Indian Ocean). *Ann. South African Museum* 98, 1-27.
- Frimmel, H.E.; Fölling, P.G.; Diamond, R. (2001). Metamorphism of the Permo-Triassic Cape Fold Belt and its basement. *South Africa. Mineral. Petrol.*, 73, 325-346.
- Frimmel, H.E. (in press). Formation of a late Mesoproterozoic supercontinent: The South Africa - East Antarctica connection. In: Condie, K.C.; Veenstra, F. (eds.) *Tempos and Events in Precambrian Time*, Elsevier, Amsterdam.

- Fullerton, L.G.; Frey, H.V.; Roark, J.H.; Thomas, H.H. (1989), Evidence for a remanent contribution in Magsat data from the Cretaceous Quiet Zone in the South Atlantic. *Geophys. Res. Lett.*, 16, 1085-1088.
- Gohl, K.; Uenzelmann-Neben, G. (2001), The crustal role of the Agulhas Plateau, southwest Indian Ocean: evidence from seismic profiling. *Geophys. J. Int.* 144, 632-646.
- Inkaba ye Africa (2003), A joint initiative of the German and South African Earth Science Communities.
- Jokat, W.; Boebel, T.; König, M.; Meyer, U. (2003). Timing and geometry of early Gondwana break-up. *J. Geophys. Res.*, 108, 2428, doi: 10.1019/2002JB001802.
- Kristoffersen, Y.; LaBrecque, J.L. (1991), On the tectonic history and origin of the Northeast Georgia Rise. In: Ciesielski, P.F., Y. Kristoffersen et al. (eds.) *Proc. ODP, Sci. Results*, 114, College Station, Tx (Ocean Drilling Program), 23-38.
- LaBrecque, J.L.; Hayes, D.E. (1979), Seafloor spreading history of the Agulhas Basin. *Earth and Planetary Science Letters*, 45, 411-428.
- Lyakhovsky, V.; Ben-Avraham, Z.; Reznikov, M. (1994), Stress distribution over the Mozambique Ridge. *Tectonophysics*, 240, 21-27.
- McMillan, I.K., Brink, G.J., Broad, D.S. & Maier, J.J. (1997). Late Mesozoic sedimentary basins off the south coast of South Afrika. In: Selley, R.C. (Ed.), *Sedimentary Basins of the World: The African Basins*. Elsevier, Amsterdam, 319-376.
- Marks, K.M.; Stock, J.M. (2001), Evolution of the Malvinas Plate south of Africa. *Marine Geophys. Res.*, 22, 289-302.
- Marks, K.M.; Tikku, A.A. (2001), Cretaceous reconstructions of East Antarctica, Africa and Madagascar. *Earth and Planetary Science Letters*, 186, 479-495.
- Martin, A.K. (1987), Plate reorganisations around Southern Africa, hotspots and extinctions. *Tectonophysics*, 142, 309-316.
- Martin, A.K.; Hartnady, C.J.H. (1986), Plate tectonic development of the southwest Indian Ocean: A revised reconstruction of East Antarctica and Africa. *Journal Geophys. Research*, 91, 4767-4786.
- Mougenot, D.; Genesseeux, M.; Hernandez, J.; Lepvrier, C.; Mallod, J.-A.; Raillard, S.; Vanney, J.-R.; Villeneuve, M. (1991). La ride du Mozambique (Ocean Indien): un fragment continental individualise lors du coulisement de l'Amerique et de l'Antarctique le long de l'Afrique de l'Est? *C. R. Acad. Sci. Paris, Ser. II* 312, 655-662.
- Niemi, T.; Ben-Avraham, Z.; Hartnady, C.J.H.; Reznikov, M. (2000). Post-Eocene seismic stratigraphy of the deep ocean basin adjacent to the southeast African continental margin: A record of geostrophic bottom current systems. *Marine Geology*, 162, 237-258.
- Raillard, S. (1990), Les Marges de l'Afrique de l'est et les Zones de Fracture associée: Chaîne Davie et Ride du Mozambique. PhD thesis, University Pierre et Marie Curie, Paris.
- Reznikov, M.; Ben-Avraham, Z.; Hartnady, C.; Niemi, T.M. (2005). Structure of the Transkei

- Basin and Natal Valley, Southwest Indian Ocean, from seismic reflection and potential field data. *Tectonophysics*, 397, 127-141.
- Richardson, P.L.; Lutjeharms, J.R.E.; Boebel, O. (2002), Introduction to the „Inter-ocean exchange around southern Africa“. *Deep-sea Research II*, 50, 1-12.
- Sandwell, D.T.; Smith, W.H.F. (1997). Marine gravity anomaly from Geosat and ERS 1 satellite altimetry. *J. Geophys. Res.*, 102, 10039-10054.
- Spieß, V. (1993): *Digitale Sedimentechographie.- Neue Wege zu einer hochauflösenden Akustostratigraphie.- Berichte, Fachbereich Geowissenschaften, Universität Bremen*, 35, 199 pp.
- Tikku, A.A.; Marks, K.M.; Kovacs, L.C. (2002). An Early Cretaceous extinct spreading center in the northern Natal Valley. *Tectonophysics*, 347, 87-108.
- Tucholke, B.E.; Carpenter, G.B. (1977), Sedimentary distribution and Cenozoic sedimentation patterns on the Agulhas Plateau. *Geological Society of America Bulletins*, 88, 1337- 1346.
- Tucholke, B.; Embley, R.E. (1984), Cenozoic regional erosion of the abyssal sea floor off South Africa. In: Schlee, J.S. (ed.) *Interregional unconformities and hydrocarbon accumulation*, AAPG Memoir, 36, 145-164.
- Tucholke, B.E.; Houtz, R.E.; Barrett, D.M. (1981), Continental crust beneath the Agulhas Plateau, southwest Indian Ocean. *Journal of Geophysical Research*, 86, 3791-38061.
- Uenzelmann-Neben, G. (2001). Seismic characteristics of sediment drifts: An example from the Agulhas Plateau, southwest Indian Ocean, *Marine Geophysical Researches*, 22, 323-343.
- Uenzelmann-Neben, G. (2003). Contourites on the Agulhas Plateau, SW Indian Ocean: Indications for the evolutions of currents since Palaeogene times. In: Stow, D., Pudsey, C., Howe, J., Faugeres, J.C., Viana, A.R. (eds), *Deep-water contourite systems: Modern drifts and ancient series*. Geological Society of London, Memoir, 22, 271-288.
- Uenzelmann-Neben, G.; Gohl, K.; Ehrhardt, A.; Seargent, M. (1999). Agulhas Plateau, SW Indian Ocean: New evidence for excessive volcanism, *Geophysical Research Letters*, 26/13, 1941-1944.
- Wessel, P.; W.H.F. Smith (1998) New improved version of Generic Mapping Tools released. *EOS Trans. Amer. Geophys. U*, 79, 579.

Appendix I: Seismic profile parameters

Line	begin			end			length [nm]	airgun config.	total volume [l]	shot interval [s]	No of shots	field tapes
	time in UTC	lat	lon	time in UTC	lat	lon						
AWI-20050001	14.4.05 04:30:30	-35.6645	24.5000	17.4.05 07:44:30	-35.6671	31.33883	333	3 GI-guns	7.2	10	27084	F07213- F07215, F07217- F07241
AWI-20050002	17.4.05 09:44:10	-35.6521	31.3192	17.4.05 18:45:30	-36.1428	30.63429	44	3 GI-guns	7.2	10	3248	F07242- F07245
AWI-20050003	17.4.05 20:24:30	-36.1727	30.6884	18.4.05 10:54:00	-35.0009	30.49688	71	3 GI-guns	7.2	10	5217	F07246- F07251
AWI-20050004	18.4.05 15:39:00	-35.0904	30.4954	19.4.05 04:37:00	-36.1203	30.32508	62	3 GI-guns	7.2	10	4668	F07253- F07256
AWI-20050005	19.4.05 06:26:00	-36.1211	30.3219	19.4.05 19:51:10	-34.9997	30.14487	68	3 GI-guns	7.2	10	4831	F07258- F07261
AWI-20050006	19.4.05 21:43:00	-35.0323	30.1505	20.4.05 07:42:20	-35.7742	30.02958	45	3 GI-guns	7.2	10	3596	F07263- F07266
AWI-20050007	30.4.05 15:20:50	-36.078	29.9643	01.5.05 03:25:00	-35.0341	29.7596	63	3 GI-guns	7.2	10	4345	F07271- F07274
AWI-20050008	01.5.05 03:43:30	-35.0335	29.7352	01.5.05 19:19:00	-36.121	29.5914	66	3 GI-guns	7.2	10	5613	F07275- F07280
AWI-20050009	01.5.05 19:56:00	-36.1186	29.5584	02.5.05 08:32:00	-35.0320	29.394	66	3 GI-guns	7.2	10	4536	F07280- F07284
AWI-20050010	02.5.05 08:50:00	-35.0312	29.3733	02.5.05 22:13:00	-36.1213	29.2369	66	3 GI-guns	7.2	10	4818	F07285- F07288
AWI-20050011	02.5.05 22:54:00	-36.1199	29.2094	03.5.05 14:39:30	-35.03348	29.0568	66	3 GI-guns	7.2	10	5673	F07289- F07293
AWI-20050012	03.5.05 14:54:00	-35.0352	29.0366	04.5.05 04:13:00	-36.1204	28.9116	66	3 GI-guns	7.2	10	4794	F07294- F07298
AWI-	04.5.05	-36.1203	28.8907	04.5.05	-35.7746	28.6678	24	3 GI-guns	7.2	10	1754	F07299-

Appendix II: OBS station list, profile AWI-20050100

OBS station coordinates of profile AWI-20050100

stat. No.	OBS/H type	deployment					recovery				
		date	UTC	latitude S	longitude E	water depth m	date	UTC	latitude S	longitude E	water depth m
101	OBS 3-foot	08.04.2005	10:16	37° 17.902'	24° 18.058'	4711	12.04.2005	10:02	37° 16.456'	24° 20.220'	4636
102	OBS 3-foot	08.04.2005	11:20	37° 08.115'	24° 12.291'	4873	12.04.2005	12:08	37° 07.402'	24° 12.881'	4849
103	OBS 3-foot	08.04.2005	12:31	36° 58.186'	24° 06.593'	4970	12.04.2005	13:37	36° 57.870'	24° 06.940'	4933
104	OBS 3-foot	08.04.2005	13:32	36° 48.318'	24° 01.198'	5008	12.04.2005	15:01	36° 48.108'	24° 01.311'	4973
105	OBS 3-foot	08.04.2005	14:35	36° 38.508'	23° 55.431'	4865	12.04.2005	16:33	36° 38.384'	23° 55.600'	4830
106	OBS flat	08.04.2005	15:32	36° 29.018'	23° 50.151'	4236	12.04.2005	18:25	36° 29.212'	23° 50.107'	4215
107	OBS flat	08.04.2005	16:36	36° 19.166'	23° 44.418'	3434	12.04.2005	20:22	36° 19.530'	23° 44.617'	3755
108	OBS flat	08.04.2005	17:37	36° 09.314'	23° 39.017'	2500	12.04.2005	22:05	36° 09.530'	23° 38.660'	3759
109	OBS flat	08.04.2005	18:39	35° 59.339'	23° 33.119'	2182	13.04.2005	23:45	35° 59.788'	23° 32.142'	2124
110	OBS flat	08.04.2005	19:36	35° 49.515'	23° 27.536'	2156	13.04.2005	01:19	35° 50.218'	23° 25.879'	2133
111	OBS flat	08.04.2005	20:30	35° 40.095'	23° 22.546'	1965	13.04.2005	02:54	35° 40.819'	23° 20.208'	2042
112	OBS flat	08.04.2005	21:30	35° 30.185'	23° 16.530'	1775	13.04.2005	04:30	35° 31.290'	23° 13.036'	1776
113	OBS flat	08.04.2005	22:44	35° 20.258'	23° 11.238'	1326	13.04.2005	06:10	35° 20.893'	23° 07.367'	1227
114	OBS flat	09.04.2005	00:17	35° 05.256'	23° 02.371'	305	13.04.2005	08:47	35° 05.209'	23° 02.531'	236
115	OBS flat	09.04.2005	01:20	34° 55.110'	22° 56.553'	155	13.04.2005	10:14	34° 55.200'	22° 56.564'	149
116	OBS flat	09.04.2005	02:11	34° 47.299'	22° 52.292'	121	13.04.2005	11:27	34° 47.360'	22° 52.245'	119
117	OBS flat	09.04.2005	02:50	34° 41.252'	22° 49.017'	118	13.04.2005	12:17	34° 41.295'	22° 48.971'	118
118	OBS flat	09.04.2005	03:48	34° 31.529'	22° 43.171'	110	13.04.2005	13:27	34° 31.577'	22° 43.074'	119
119	OBS flat	09.04.2005	04:52	34° 21.298'	22° 38.265'	93	13.04.2005	14:43	34° 21.343'	22° 38.144'	176
120	OBS flat	09.04.2005	05:27	34° 16.255'	22° 35.019'	85	13.04.2005	15:28	34° 16.301'	22° 34.897'	161

OBS recordings of profile AWI-20050100

62

stat. No.	rec. type	recorder S/N	seismometer type	seismometer S/N	sample rate Hz	recorded data MB	data quality check:				remarks
							ch 1 hyd	ch 2 X	ch 3 Y	ch 4 Z	
101	MBS	980901	Owen 4.5 Hz	03/052 no. 10	250	437	2	1-2	1-2	1-2	
102	MBS	980902	Owen 4.5 Hz	KS 0310-049 no. 19	250	0	0	0	0	0	no data (no error found; test ok)
103	MBS	000612	Owen 4.5 Hz	KS 0403-059 no. 59	250	251	?	?	?	?	recording stopped early; cannot read
104	MBS	010703	Owen 4.5 Hz	KS 0309-047 no. 26	250	436	2	2	2	2	
105	MBS	990712	Owen 4.5 Hz	KS 0310-92 no.40	250	445	2	1-2	1-2	2	
106	MBS	990901	Owen 4.5 Hz	unknown	250	469	2	1-2	1-2	2	
107	MBS	020505	Owen 4.5 Hz	KS 0403-058 no.58	250	516	2	0-1	0-1	0-1	
108	MES	030901	Owen 4.5 Hz	KS 0310 050 no. 20	250	570	2	2	2	2	
109	MBS	000614	Owen 4.5 Hz	KS 0309 045 no.24	250	452	2	2	2	2	
110	MBS	010701	Owen 4.5 Hz	KS 0307 041 no.23	250	512	2	2	2	2	
111	MBS	000613	Owen 4.5 Hz	no. 6	250	0	0	0	0	0	no data (error: burnt fuse)
112	MBS	020504	Owen 4.5 Hz	KS 0310 051 no.29	250	488	2	1-2	1-2	2	
113	MBS	020509	Owen 4.5 Hz	KS 0403 060 no.60	250	579	2	1-2	1-2	1-2	
114	MBS	001005	Owen 4.5 Hz	KS 0205 032 no.39	250	476	2	1-2	1-2	2	
115	MBS	001002	Owen 4.5 Hz	0310-0848 no.27	250	351	2	1-2	1-2	1-2	
116	MBS	980903	Owen 4.5 Hz	KS 0202-022 no.22	250	554	1	0-1	0-1	0-1	
117	MBS	020506	Owen 4.5 Hz	KS 0310-053 no.41	250	447	2	0-1	0-1	1	
118	MBS	991292	Owen 4.5 Hz	40864	250	505	2	0-1	0-1	1	
119	MBS	020501	Owen 4.5 Hz	KS 0403-057 no.57	250	416	0-1	2	2	2	seconds pulse on ch. 4
120	MBS	980906	Owen 4.5 Hz	no.5	250	458	2	2	2	2	

RV Sonne So-182 Cruise Report

AISTEK-1

Uenzelmann-Neben

Appendix III: Land station and shot list, profile AWI-20050100

Seismic Land Profile 1 Frazerburg - Heroldsbay
Shot List

No.	Latitude South	Longitude East	Elev. (m)	date	h UTC	m	sec	Charge (kg)
1	33.99758	22.39000	193	09.04.05	10	47	9.2240	250
2	33.86654	22.33842	702	09.04.05	12	44	45.3620	250
3	33.69451	22.27251	472	09.04.05	14	31	16.3720	200
4	33.55233	22.20567	467	10.04.05	6	40	2.0419	200
5	33.39040	22.13930	788	10.04.05	8	50	44.5549	150
6	33.21691	22.07177	596	10.04.05	11	36	54.7280	150
7	33.01792	21.98391	482	10.04.05	13	15	45.1740	150
8	32.87182	21.91580	566	11.04.05	5	51	50.5240	150
9	32.67119	21.84170	635	11.04.05	7	41	25.9660	150
10	32.47676	21.76296	716	11.04.05	9	21	11.2156	200
11	32.34512	21.70386	913	11.04.05	11	2	4.9220	200
12	32.16307	21.62175	1452	11.04.05	12	50	53.7180	250
13	32.01766	21.56335	1342	11.04.05	14	55	28.1640	250

Seismic Land Profile 1 Frazerburg - Heroldsbay
Station List

Station No.	Latitude South	Longitude East	Elevation (m)
1	32.04955	21.58273	1372
2	32.08959	21.59693	1465
3	32.12972	21.61472	1477
4	32.17583	21.63306	1435
5	32.22189	21.65047	1153
6	32.27453	21.67938	1103
7	32.30111	21.68639	1001

8	32.34473	21.70369	898
9	32.38266	21.71791	852
10	32.42400	21.74008	767
11	32.47619	21.76303	730
12	32.51722	21.77972	701
13	32.56616	21.79840	670
14	32.61584	21.82102	626
15	32.66955	21.84184	627
16	32.70567	21.85654	639
17	32.73418	21.86611	632
18	32.77356	21.88089	613
19	32.80665	21.89988	596
20	32.87153	21.91581	589
21	32.89309	21.93353	602
22	32.94536	21.95231	542
23	32.99064	21.97183	526
24	33.02420	21.98847	438
25	33.06750	22.00528	534
26	33.11330	22.02232	611
27	33.14365	22.03816	600
28	33.19744	22.06014	594
29	33.23700	22.07340	688
30	33.27526	22.08022	838
31	33.33135	22.11030	1662
32	33.38531	22.13765	742
33	33.47689	22.16500	537
34	33.50387	22.18958	519
35	33.54654	22.20453	421
36	33.57927	22.22238	423
37	33.61718	22.23737	322
38	33.65760	22.25777	564
39	33.69492	22.26977	456
40	33.74245	22.29248	470
41	33.77886	22.30448	504

42	33.79735	22.31303	556
43	33.85062	22.33412	626
44	33.87726	22.34629	638
45	33.91263	22.36180	444
46	33.95865	22.37474	246
47	33.99800	22.39068	177
48	34.04344	22.40620	196

Appendix IV: OBS station list, profile AWI-20050200

OBS station coordinates of profile AWI-20050200

stat. No.	OBS/H type	deployment					recovery				
		date	UTC	latitude S	longitude E	water depth m	date	UTC	latitude S	longitude E	water depth m
201	OBS 3-foot	22.04.2005	07:30	40° 06.983'	26° 16.444'	2494	27.04.2005	07:32	40° 05.682'	26° 13.277'	2450
202	OBS 3-foot	22.04.2005	08:41	39° 53.368'	26° 13.243	2510	27.04.2005	09:03	39° 52.682'	26° 11.550'	2478
203	OBS flat	22.04.2005	09:48	39° 40.181'	26° 10.091'	2500	27.04.2005	10:46	39° 39.805'	26° 09.008'	2465
204	OBS 3-foot	22.04.2005	10:56	39° 27.044'	26° 05.507'	2453	27.04.2005	12:16	39° 26.894'	26° 05.337'	2432
205	OBS 3-foot	22.04.2005	12:09	39° 13.528'	26° 03.266'	2414	27.04.2005	14:25	39° 13.390'	26° 02.432'	2393
206	OBH	22.04.2005	13:21	39° 00.313'	26° 00.096'	2601	27.04.2005	16:21	39° 00.384'	25° 59.105'	2596
207	OBS 3-foot	22.04.2005	14:35	38° 47.111'	25° 56.474'	2878	27.04.2005	17:59	38° 46.979'	25° 55.269'	2862
208	OBS 3-foot	22.04.2005	15:48	38° 33.511'	25° 53.330'	2925	27.04.2005	19:21	38° 33.429'	25° 52.919'	2891
209	OBS flat	22.04.2005	16:58	38° 20.347'	25° 50.129'	3150	27.04.2005	21:10	38° 20.366'	25° 49.881'	3144
210	OBS 3-foot	22.04.2005	18:07	38° 07.138'	25° 46.555'	3016	27.04.2005	22:37	38° 07.125'	25° 46.625'	2996
211	OBS 3-foot	22.04.2005	19:18	37° 53.540'	25° 43.377'	3123	28.04.2005	00:30	37° 53.565'	25° 43.602'	3099
212	OBS flat	22.04.2005	20:27	37° 40.327'	25° 40.134'	3130	28.04.2005	02:42	37° 40.157'	25° 40.496'	3075
213	OBS 3-foot	22.04.2005	21:31	37° 27.114'	25° 36.588'	2956	28.04.2005	04:10	37° 26.984'	25° 36.945'	2921
214	OBS 3-foot	22.04.2005	22:37	37° 14.039'	25° 33.299'	3270	28.04.2005	05:48	37° 14.059'	25° 33.555'	3245
215	OBS flat	22.04.2005	23:52	37° 00.475'	25° 30.217'	3544	28.04.2005	08:00	37° 00.557'	25° 30.680'	-
216	OBS 3-foot	23.04.2005	01:07	36° 47.260'	25° 26.323'	3678	28.04.2005	10:50	36° 47.327'	25° 27.221'	3702
217	OBS flat	23.04.2005	02:24	36° 34.099'	25° 23.367'	4118	28.04.2005	13:03	36° 34.671'	25° 24.729'	-
218	OBS flat	23.04.2005	03:39	36° 20.496'	25° 20.158'	3479	28.04.2005	15:03	36° 20.383'	25° 20.989'	3515
219	OBS flat	23.04.2005	04:50	36° 07.231'	25° 16.634'	4844	28.04.2005	17:40	36° 07.321'	25° 16.959'	-
220	OBS flat	23.04.2005	05:59	35° 54.070'	25° 13.396'	4758	28.04.2005	19:49	35° 54.163'	25° 13.530'	-
221	OBS flat	23.04.2005	07:10	35° 40.495'	25° 10.200'	4572	28.04.2005	22:05	35° 40.634'	25° 09.758'	-
222	OBS flat	23.04.2005	08:22	35° 27.305'	25° 07.013'	4188	29.04.2005	00:26	35° 27.795'	25° 05.085'	-
223	OBS flat	23.04.2005	09:39	35° 14.142'	25° 03.411'	2709	29.04.2005	02:21	35° 14.464'	25° 02.204'	-
224	OBS flat	23.04.2005	10:59	35° 00.573'	25° 00.184'	1805	29.04.2005	04:04	35° 00.965'	24° 58.167'	1771
225	OBS flat	23.04.2005	12:14	34° 48.540'	24° 57.059'	503	29.04.2005	05:29	34° 48.979'	24° 55.565'	-
226	OBS flat	23.04.2005	14:05	34° 28.158'	24° 51.581'	126	29.04.2005	07:38	34° 28.215'	24° 51.382'	123
227	OBS flat	23.04.2005	14:47	34° 21.032'	24° 50.296'	130	29.04.2005	08:36	34° 21.04'	24° 50.19'	126

OBS recordings of profile AWI-20050200

stat. No.	rec. type	recorder S/N	seismometer type	seismometer S/N	sample rate Hz	recorded data MB	data quality check: 0 = no data 1 = short offset arrivals 2 = large offset arrivals				remarks
							ch 1 hyd	ch 2 X	ch 3 Y	ch 4 Z	
201	MBS	001002	Owen 4.5 Hz	MDGE 03/04	250	530	2	2	2	2	
202	MBS	991292	Owen 15 Hz	no.30	250	513	2	2	2	2	
203	MBS	020506	Owen 4.5 Hz	no.60	250	647	1-2	1	1	1	
204	MBS	020509	Owen 4.5 Hz	KS 0309-047 no.26	250	529	2	2	2	2	
205	MBS	980903	Owen 4.5 Hz	no.6	250	519	1-2	2	2	2	
206	MES	030901	n/a	n/a	250	223	1	n/a	n/a	n/a	
207	MES	031002	Owen 4.5 Hz	no.7	250	785	2	2	2	2	
208	MBS	980906	Owen 4.5 Hz	no.2	250	550	2	2	2	2	
209	MBS	001005	Owen 4.5 Hz	no.24	250	815	1	0	0	0	
210	MBS	010701	Owen 15 Hz	no.39	250	545	2	2	2	2	
211	MBS	020501	Owen 4.5 Hz	no.59	250	555	2	2	2	2	
212	MBS	020504	Owen 4.5 Hz	no.19	250	546	2	2	2	2	
213	MBS	980901	Owen 4.5 Hz	no.10	250	553	2	2	2	2	
214	MBS	020505	Owen 4.5 Hz	?	250	566	2	2	2	2	
215	MBS	000613	Owen 4.5 Hz	KS 0403-055 no.55	250	579	2	2	2	2	
216	MBS	010703	Owen 4.5 Hz	MDG0305 no.8	250	565	2	0-1	0-1	0-1	seismometer was displaced at descent
217	MBS	000612	Owen 15 Hz	KS 0205-027 no.34	250	574	?	?	?	?	cannot read data
218	MBS	990712	Owen 4.5 Hz	KS 0310-051 no.29	250	585	2	2	2	2	
219	MBS	000602	Owen 4.5 Hz	KS 0310-050 no.20	250	595	2	2	2	2	
220	MBS	980909	Owen 4.5 Hz	KS 0202-022 no.22	250	604	2	2	2	2	
221	MBS	980908	Owen 4.5 Hz	KS 0310-048 no.27	250	617	1-2	1-2	1-2	1-2	
222	MBS	000611	Owen 4.5 Hz	0403-057 no.57	250	560	0-1	1-2	1-2	1-2	
223	MBS	000616	Owen 15 Hz	KS 0205-025 no.32	125	296	1-2	0	0	0	
224	MBS	001006	Owen 4.5 Hz	KS 0307-041 no.23	250	686	2	1	1	1	
225	MBS	001004	Owen 4.5 Hz	KS 0403-058 no.58	250	562	1	0	0	0	

226	MES	030902	Owen 4.5 Hz	no.64	250	890	1-2	0-1	0-1	0-1	0-1	0-1	0-1
227	MES	030905	Owen 4.5 Hz	KS 0310-053 no.41	250	909	?	?	?	?	?	?	cannot read data
trigg.	MBS	001001	n/a	n/a	62.5	20	ok	n/a	n/a	n/a	n/a	n/a	n/a

Appendix V: Land station and shot list, profile AWI-20050300

Seismic Land Profile 2 Graaf Reinet – Cape St. Francis
Shot List

No.	Latitude South	Longitude East	Elev. (m)	date	h UTC	m	sec	Charge (kg)
13	32.32425	24.58266	725	24.04.05	9	1	15.8323	250
12	32.48522	24.60923	661	24.04.05	10	56	19.6826	250
11	32.62487	24.62538	579	24.04.05	14	21	19.4271	200
10	32.76393	24.64347	512	24.04.05	16	4	25.5509	200
9	32.95579	24.66823	472	25.04.05	7	41	17.0519	150
8	33.12369	24.69035	480	25.04.05	9	11	16.1080	150
7	33.25456	24.70828	523	25.04.05	11	6	14.9540	150
6	33.43344	24.73091	343	25.04.05	13	6	17.2020	150
5	33.63685	24.75505	714	26.04.05	7	46	16.9202	150
4	33.77400	24.76781	180	25.04.05	10	3	34.3713	200
3	33.88585	24.78515	343	25.04.05	12	1	40.2974	200
2	34.06548	24.80606	77	25.04.05	13	41	14.0720	250
1	34.12071	24.81516	71	25.04.05	14	56	13.9461	250

Seismic Land Profile 2 Graaf Reinet – Cape St. Francis
Station List

Station No.	Latitude South	Longitude East	Elevation (m)
47	34.20247	24.82166	45
46	34.15538	24.82024	27
45	34.12362	24.81497	40
44	34.08644	24.81274	58
43	34.06224	24.80382	38
42	34.03040	24.79922	163
41	33.98330	24.79908	247
40	33.96497	24.79907	259

39	33.92438	24.79218	277
38	33.88445	24.78692	344
37	33.82547	24.77987	384
36	33.77032	24.77067	83
35	33.72788	24.76422	33
34	33.66648	24.75959	599
33	33.63697	24.75490	728
32	33.51411	24.73951	418
31	33.47325	24.73531	357
30	33.43692	24.73080	338
29	33.40539	24.72823	379
28	33.35323	24.72018	452
27	33.31309	24.71684	529
26	33.25955	24.70908	562
25	33.22945	24.72239	650
24	33.16746	24.69659	548
23	33.12177	24.69048	497
22	33.09246	24.68559	479
21	33.07568	24.68395	454
20	33.03457	24.67878	489
19	32.98953	24.67091	444
18	32.95661	24.66809	439
17	32.92370	24.66147	446
16	32.89549	24.66041	453
15	32.85704	24.65418	471
14	32.81102	24.64786	493
13	32.76984	24.64397	513
12	32.74327	24.64089	534
11	32.69780	24.63551	565
10	32.66742	24.63071	572
09	32.62435	24.62535	581
08	32.58281	24.61949	604
07	32.54413	24.61620	609
06	32.51810	24.61311	653

05	32.48570	24.60942	667
04	32.44161	24.60326	705
03	32.40913	24.60000	725
02	32.36497	24.59037	713
01	32.3232	24.58192	667

Appendix VI: OBS station list, profile AWI-20050300

OBS station coordinates of profile AWI-20050300

stat. No.	OBS/H type	deployment					recovery				
		date	UTC	latitude S	longitude E	water depth m	date	UTC	latitude S	longitude E	water depth m
301	OBS flat	08.05.2005	15:28	35° 29,976'	32° 42,012'	3919	11.05.2005	9:24	35° 30,265'	32° 42,169'	-
302	OBS flat	08.05.2005	18:20	35° 18,384'	32° 47,237'	2965	11.05.2005	11:07	35° 18,685'	32° 47,580'	-
303	OBS flat	08.05.2005	21:12	35° 07,182'	32° 52,458'	3186	11.05.2005	12:51	35° 07,074'	32° 53,005'	-
304	OBS flat	09.05.2005	00:02	34° 55,982'	32° 57,984'	2871	11.05.2005	14:34	34° 55,766'	32° 58,615'	-
305	OBS flat	09.05.2005	02:31	34° 44,412'	33° 03,191'	2324	11.05.2005	16:49	34° 44,022'	33° 04,052'	-
306	OBS flat	09.05.2005	04:50	34° 33,222'	33° 08,376'	2400	11.05.2005	18:21	34° 32,954'	33° 08,735'	-
307	OBS flat	09.05.2005	07:08	34° 21,963'	33° 14,008'	2043	11.05.2005	19:48	34° 21,484'	33° 14,131'	-
308	OBS flat	09.05.2005	09:08	34° 10,350'	33° 19,189'	1581	11.05.2005	21:11	34° 09,966'	33° 19,010'	-
309	OBS flat	09.05.2005	11:46	33° 59,010'	33° 24,484'	1895	11.05.2005	23:22	33° 57,537'	33° 22,944'	-
310	OBS flat	09.05.2005	13:40	33° 47,981'	33° 30,000'	2037	12.05.2005	0:47	33° 47,519'	33° 29,569'	-

OBS recordings of profile AWI-20050300

stat. No.	rec. type	recorder S/N	seismometer type	seismometer S/N	sample rate Hz	recorded data MB	data quality check:				remarks
							ch 1 hyd	ch 2 X	ch 3 Y	ch 4 Z	
301	MBS	010701	Owen 4,5 Hz	no.55	250	353	1-2	0-1	0-1	0-1	
302	MBS	001006	Owen 4,5 Hz	no.59	250	311	2	1-2	1-2	1-2	
303	MBS	010703	Owen 4,5 Hz	no.34	250	344	?	?	?	?	cannot read data
304	MBS	980901	Owen 4,5 Hz	no.29	250	292	2	2	2	2	
305	MBS	000613	Owen 4,5 Hz	KS 0310-048 no.27	250	313	1-2	1	1	1	coherent noise on ch. 1
306	MBS	010109	Owen 4,5 Hz	KS 0202-022 no. 22	250	329	2	1-2	1-2	1-2	

307	MBS	000614	Owen 4,5 Hz	KS 0307-041 no.23	250	287	2	2	2	2	2	2	no records (programming error)
308	MBS	020505	Owen 4,5 Hz	no.20	250	0	0	0	0	0	0	0	
309	MBS	020501	Owen 4,5 Hz	KS 0310-053 no. 41	250	310	2	2	2	2	2	2	
310	MBS	001003	Owen 4,5 Hz	KS 0403-060 no.60	250	292	2	1-2	1-2	1-2	1-2	2	
trigg.	MBS	001001	n/a	n/a	250	31	ok	n/a	n/a	n/a	n/a	n/a	

"Berichte zur Polarforschung"

Eine Titelübersicht der Hefte 1 bis 376 (1981 - 2000) erschien zuletzt im Heft 413 der nachfolgenden Reihe "Berichte zur Polar- und Meeresforschung". Ein Verzeichnis aller Hefte beider Reihen sowie eine Zusammenstellung der Abstracts in englischer Sprache finden sich im Internet unter der Adresse:

<http://www.awi-bremerhaven.de/Resources/publications.html>

Ab dem Heft-Nr. 377 erscheint die Reihe unter dem Namen: "Berichte zur Polar- und Meeresforschung".

- Heft-Nr. 377/2000** – „Rekrutierungsmuster ausgewählter Wattfauna nach unterschiedlich strengen Wintern“ von Matthias Strasser.
- Heft-Nr. 378/2001** – „Der Transport von Wärme, Wasser und Salz in den Arktischen Ozean“, von Boris Cisewski.
- Heft-Nr. 379/2001** – „Analyse hydrographischer Schnitte mit Satellitenaltimetrie“, von Martin Losch.
- Heft-Nr. 380/2001** – „Die Expeditionen ANTARKTIS XVI/1-2 des Forschungsschiffes POLARSTERN 1998/1999“, herausgegeben von Eberhard Fahrbach und Saad El Naggar.
- Heft-Nr. 381/2001** – „UV-Schutz- und Reparaturmechanismen bei antarktischen Diatomeen und *Phaeocystis antarctica*“, von Lieselotte Riegger.
- Heft-Nr. 382/2001** – „Age determination in polar Crustacea using the autofluorescent pigment lipofuscin“, by Bodil Bluhm.
- Heft-Nr. 383/2001** – „Zeitliche und räumliche Verteilung, Habitatspräferenzen und Populationsdynamik benthischer Copepoda Harpacticoida in der Potter Cove (King George Island, Antarktis)“, von Gritta Veit-Köhler.
- Heft-Nr. 384/2001** – „Beiträge aus geophysikalischen Messungen in Dronning Maud Land, Antarktis, zur Auffindung eines optimalen Bohrpunktes für eine Eiskerntiefbohrung“, von Daniel Steinhage.
- Heft-Nr. 385/2001** – „Actinium-227 als Tracer für Advektion und Mischung in der Tiefsee“, von Walter Geibert.
- Heft-Nr. 386/2001** – „Messung von optischen Eigenschaften troposphärischer Aerosole in der Arktis“, von Rolf Schumacher.
- Heft-Nr. 387/2001** – „Bestimmung des Ozonabbaus in der arktischen und subarktischen Stratosphäre“, von Astrid Schulz.
- Heft-Nr. 388/2001** – „Russian-German Cooperation SYSTEM LAPTEV SEA 2000: The Expedition LENA 2000“, edited by Volker Rachold and Mikhail N. Grigoriev.
- Heft-Nr. 389/2001** – „The Expeditions ARKTIS XVI/1 and ARKTIS XVI/2 of the Research Vessel ‚Polarstern‘ in 2000“, edited by Gunther Krause and Ursula Schauer.
- Heft-Nr. 390/2001** – „Late Quaternary climate variations recorded in North Atlantic deep-sea benthic ostracodes“, by Claudia Didié.
- Heft-Nr. 391/2001** – „The polar and subpolar North Atlantic during the last five glacial-interglacial cycles“, by Jan P. Helmke.
- Heft-Nr. 392/2001** – „Geochemische Untersuchungen an hydrothermal beeinflussten Sedimenten der Bransfield Straße (Antarktis)“, von Anke Dähmann.
- Heft-Nr. 393/2001** – „The German-Russian Project on Siberian River Run-off (SIRRO): Scientific Cruise Report of the Kara-Sea Expedition ‚SIRRO 2000‘ of RV ‚Boris Petrov‘ and first results“, edited by Ruediger Stein and Oleg Stepanets.
- Heft-Nr. 394/2001** – „Untersuchungen der Photooxidantien Wasserstoffperoxid, Methylhydroperoxid und Formaldehyd in der Troposphäre der Antarktis“, von Katja Riedel.
- Heft-Nr. 395/2001** – „Role of benthic cnidarians in the energy transfer processes in the Southern Ocean marine ecosystem (Antarctica)“, by Covadonga Orejas Saco del Valle.
- Heft-Nr. 396/2001** – „Biogeochemistry of Dissolved Carbohydrates in the Arctic“, by Ralph Engbrodt.
- Heft-Nr. 397/2001** – „Seasonality of marine algae and grazers of an Antarctic rocky intertidal, with emphasis on the role of the limpet *Nacilla concinna* Strebel (Gastropoda: Patellidae)“, by Dohong Kim.
- Heft-Nr. 398/2001** – „Polare Stratosphärenwolken und mesoskalige Dynamik am Polarwirbelrand“, von Marion Müller.
- Heft-Nr. 399/2001** – „North Atlantic Deep Water and Antarctic Bottom Water: Their Interaction and Influence on Modes of the Global Ocean Circulation“, by Holger Brix.
- Heft-Nr. 400/2001** – „The Expeditions ANTARKTIS XVIII/1-2 of the Research Vessel ‚Polarstern‘ in 2000“, edited by Victor Smetacek, Ulrich Bathmann, Saad El Naggar.
- Heft-Nr. 401/2001** – „Variabilität von CH₂O (Formaldehyd) - untersucht mit Hilfe der solaren Absorptionsspektroskopie und Modellen“, von Torsten Albrecht.
- Heft-Nr. 402/2001** – „The Expedition ANTARKTIS XVII/3 (EASIZ III) of RV ‚Polarstern‘ in 2000“, edited by Wolf E. Arntz and Thomas Brey.
- Heft-Nr. 403/2001** – „Mikrohabitatansprüche benthischer Foraminiferen in Sedimenten des Südatlantiks“, von Stefanie Schumacher.